The Pacific Ocean Heat Engine

Supplementary Information

Roger N Jones and James H Ricketts

S1. Testing for shifts

S1.1. Detection: The multi-step bivariate test

The main method used for detecting shifts is the multi-step bivariate test MSBV (Ricketts, 2015;Ricketts and Jones, 2016;Jones and Ricketts, 2021). This is described fully in Jones and Ricketts (2017; JR17), mainly in the SI, so will not be repeated here. One small adjustment was made in the screening pass that follows the detection routine, re-checking the first change point in the sequence to ensure it remained valid in the light of later results.

Mean step changes in climate data may either be of climatic origin or due to artificial inhomogeneities, so it is important to be able to distinguish between the two. The data used in this study contains both aspects.

For historical data, the reliability of the bivariate test has been confirmed through its use in inhomogeneity testing where the test has been used to detect breaks confirmed by metadata (Potter, 1981;Bücher and Dessens, 1991;Kirono and Jones, 2007;Štěpánek et al., 2009). Once a certain level of reliability has been established, undocumented breaks can be assessed. This may prompt a search for further documentation that if located, can confirm the assessment. Although inhomogeneity testing is becoming more sophisticated, requiring a series of tests to detect different types of inhomogeneity from annual to sub-daily data (Domonkos et al., 2012;Ribeiro et al., 2016), the bivariate test is routinely used in stand-alone mode and in packages such as AnClim (Štěpánek, 2007) and is most suitable for annual to monthly data (the latter applied carefully).

The test has been less frequently used for detecting steplike change in climate, although the first author has been using it to detect regime shifts for almost thirty years. Historical shifts in climate have been attributed in the following ways:

- Shifts showing regional homogeneity with no artificial cause such as wholesale instrument change (Buishand, 1984;Lettenmaier et al., 1994;Vivès and Jones, 2005).
- Shifts across correlated variables that represent physical processes, also showing regional homogeneity (Boucharel et al., 2009;Boucharel et al., 2011;Jones, 2012).

- Shifts in impacts coinciding with known regime changes where downstream impacts are traced back to climatic drivers (Mantua et al., 1997;Overland et al., 2008;Reid and Beaugrand, 2012;Rodionov, 2015;Reid et al., 2016;Beaugrand et al., 2019).

The last two tasks may also be carried out using climate model output. However, this is resource intensive, requiring the analysis of multiple variables, climate indices and/or impact modelling, so is rarely attempted.

S1.2. Test limits and assumptions

In JR17 we showed that historical climate is dominated by shifts, with shift/total warming ratios of regional and zonal climates commonly in the range of 0.7 to 1.0. Under increased forcing the pattern of warming becomes more trend-like, therefore the MSBV becomes less reliable (Jones and Ricketts, 2021). These limits need to be tested. For observed climate, the possibility of trending behaviour, spatially overlapping regime shifts and memory effects also need to be tested for. An important part of testing is model specification, ensuring that statistical models are suitable for the data they test and adequately represent the hypotheses they are testing. Mayo and Spanos (2004) differentiate between model specification and model selection (and we follow them in this). They say, "Far from increasing error rates, multiple tests, if appropriate, may serve to cross-validate and fortify other tests, so that the model inferred as statistically adequate has passed a reliable test." Here, the test has already been specified and passed a series of severe tests with probative criteria showing that warming is dominated by step-like rather than trend-like processes (Jones and Ricketts, 2021).

To further assess the limits of the bivariate test, particularly under greater forcing, and to increase general confidence in its performance, a series of tests have been developed to assess whether any detected shifts are compromised by features within time series that would lead to false positives. These include tests for stationarity and trends either side of a shift. Undetected shifts may also be present.

Issues for detection of features within time series include model suitability (whether the appropriate functional form is represented) and data suitability. Issues include selection of a particular model family, and within each family (e.g., representing single, multiple or segmented regressions, or those containing discontinuities) whether too many or too few variables have been used (Mayo and Spanos, 2004). An important assumption of both the bivariate test and most models used in trend analysis is that data is independent and identically distributed. For step change detection issues, are the potential presence of deterministic trends, autocorrelation and non-deterministic features such as red noise. However, the bivariate test is robust in the face of 'brownian bridges': random walks away from a steady state and back (Maronna and Yohai, 1978). Likewise, the presence of

discontinuities will pose issues for continuous trend processes (Seidel and Lanzante, 2004;Beaulieu and Killick, 2018).

The post-detection tests have therefore been developed to (a) attribute changes between internal shift and trend changes within the data, and (b) to probe the assembled multiple change points for evidence of undiagnosed features that may have deceived the MSBV. Their conclusions help to addresses the gap between the assumptions made for the purposes of change-point detection and subsequent reasoning about those change-points.

The tests developed are:

- ANOVA and ANCOVA – analysis of variance and covariance.
  The MSBV selects a change point assuming no trend. ANCOVA tests whether regression parameters either side of the change point are different from the parameters obtained from the whole segment. Below a given p-value, a discontinuity is registered from the null of no change. Above that p-value the two alternatives are judged obey the null, so the whole segment can be adequately explained using a single set of parameters. A p-value threshold of 0.05 is used for the GCM results but the whole distribution is informative. For example, $p>0.95$ would rule out a break point, and 50:50 denotes the balance of probabilities between the two. Further testing of residuals can identify the presence of non-stationarity. ANCOVA is implemented via ANOVA in R. Two ANOVA tests are run, one based on a model with data partitioned into pre or post change, the other with no change. The residuals from the separate ANOVAs are compared. ANCOVA includes an interaction term. A separate ANOVA test is applied as a cross-check.
- A set of unit-root tests applied to test for drift and various forms of serial dependence.
  - The KPSS test assumes stationarity against an alternate of non-stationarity due a presumed unit-root. The tests can be applied as a test for stationarity (KPSS-L) or trend-stationarity (KPSS-T). The former is more rigorous, because the trend test partially subsumes a step if it is present.
  - The Augmented Dickey-Fuller test (ADF) (Dickey and Fuller, 1981) for trend-stationarity has opposite polarity. It compares non-stationarity against a null of trend-stationarity after autocorrelation with multiple lags is allowed for. It is less powerful.
  - The Zivot-Andrews (ZA) test (Zivot and Andrews, 1992), attempts to locate an externally -forced change-point as a change of regression, and contrasts that with internally-generated unit root behaviour as its null. Note that if neither unit root or a

change-point is available, the test will register a change-point – this occurs when testing residuals, when a change point, unit root or neither may be present.

The tests are applied both to the initial data segments and residuals after internal trends and shifts have been subtracted. Documented effects of violations of the ruling assumptions of all tests are accounted for, and tests are discarded if the length of the segment is too short to obtain a reliable result. The tests were written in python, calling on modules based in the r statistical programming environment.

Table S1: Tests summarised with their null hypotheses and hypotheses for segment data and residuals.

Tests on data	Hypothesis	Tests on residuals	Results	Qualification
ANCOVA null	No change across shift date	N/A	No breakpoint detected	
ANCOVA hypothesis	Break-point across shift date	N/A	Breakpoint detected	
KPSS-L null KPSS-L hypothesis	Stationary Unit-root creating non-stationarity	KPSS-L null KPSS-L hypothesis	Stationary Unit-root in residuals	Expect Nonstationary if shift is real, and stationary in residuals
KPSS-T null KPSS-T hypothesis	Trend stationary Unit-root in presence of trend creating non-stationarity	KPSS-T null KPSS-T hypothesis	Trend-stationary Unit-root in presence residuals creating trend non-stationarity	Data with step may be trend-stationary. ADF would be trend stationary
ADF null	Unit root in the presence of a trend	ADF null	Unit root	Fairly insensitive and needs long segment length
ADF hypothesis	Trend stationarity	ADF hypothesis	Trend-stationary	
ZA null	Assumes unit root without a break	ZA null	Unit root	When the data are fully stationary, it will
ZA hypothesis	Detects zero or one deterministic change points	ZA hypothesis	Externally-forced breakpoint (step, trend or both)	support the ZA hypothesis

Table S2 shows classifications based on the combinations of the unit-root and serial-dependence tests. The tests are not set up to reject the MSBV but indicates those that may need further attention.

The tests from Tables S1 and S2 were applied to a subset of the zonal, hemispheric and global data from the NCDCv4.0.1. We did investigate HadCRUv3 temperatures for the study but decided not to use them because of the slightly poorer coverage of SST in the tropics. Different adjustment and error management techniques also affected autocorrelation and we wanted to remain as close to measured variability as possible. Both records contained inhomogeneities in tropical and SH SSTs around WWII and some were larger than in previous versions.

Table S2: Classifications of data segments based on post-detection tests.

Classification	**Reasoning and interpretation**
Single shift, stationary residuals	The ZA test detects the single shift in the data segment. When the residuals contain no change-point or unit root behaviour, the ZA test will also register a change point. Both KPSS tests for residuals are stationary.
Single shift, Nonstationary residuals	The ZA test rejects the step in the data segment because of the presence of behaviour interpreted as unit-root. Removing the step in both the data segment and residuals. The KPSS-T test is trend-stationary in both tests and with residuals, KPSS-L is stationary. This is consistent with a step surround by internal trends.
Single shift, N/A	The step-change detected by the MSBV is accepted without a valid ZA result because there is insufficient data to probe further (i.e., the segment is too short to provide a reliable result). The KPSS-T tests registers trends stationary in both trials and KPSS-L is stationary with residuals. This is consistent with a short segment of single-shift Nonstationary data.
Multiple, stationary	There may be a pair of steps in the data. The ZA detects unit-root behaviour in the data segment, then a step in residuals. Both KPSS tests are stationary in residuals. This indicates the potential presence of a single additional undetected change-point.
Nonstationary	The ZA test detects unit-root behaviour in both the data segment and residuals. Short segments too brief for other tests prevent further insights. Multiple change-points on top of a Nonstationary background is too complex a situation to detect with these tests.

S1.3. Severe testing update

This section provides further information and updated results from the six severe tests in . Severe testing, developed by Mayo (1996, 2005, 2018) and Mayo and Spanos (2010, 2011), is an error statistical method that combines probative criteria with statistical testing. A hypothesis needs to pass tests that its rivals fail with a high probability. The application of probative criteria makes severe testing more powerful than straightforward statistical induction. The scientific hypothesis being tested was whether radiative forcing produces abrupt or gradual climate responses over decadal timescales. Six tests were developed.

Data sets analysed for shifts with the MSBV test included observations from the UKMO, NOAA, GISS, BEST and Cowtan and Way to 2014, and model data from a 107-member ensemble from CMIP5 RCP4.5 1861–2100 (See JR2017 SI).

Annual temperature anomalies were analysed as monotonic trends, steps with no trends, and shifts with internal trends. The latter divides a timeseries into fast and slow components. The internal trends measured between change points make up the slow component and the distance between one internal trend and the next measures a shift. Total shifts in a timeseries estimates the rapid warming component and total internal trends, the gradual component. Trends are totalled regardless of their p values, most being >0.05. This prioritises trends over shifts, making the tests for shifts more severe.

To illustrate this, Fig. 1 in the main paper shows global mean surface temperature (GMST) 1880–2018 from the NCDC data used in this paper, showing total change, fast and slow components. Only one of the internal trends in GMST achieves $p<0.05$ (1997–2013). The shift to total warming ratio is 0.93, high because positive and negative trends almost cancel each other out. This ratio is higher than earlier data to 2014 in JR2017 because of the additional shift detected for 2014.

Total warming over time series is calculated in three ways: (1) taken from the start of the first internal trend to the end of the last, (2) the difference between five-year averages at either end, the sum of average temperature for each stationary period between steps. These measures contain different sampling errors, so the model data with historical forcing was tested for bias with respect to equilibrium climate sensitivity (ECS) in a 93-model ensemble from the CMIP5 RCP4.5 archive, but showed none. The results of the six tests conducted in JR2017 including their probative aspect are summarised below (Jones and Ricketts, 2021). These have been updated where possible.

Test 1: Timing and magnitude of shifts, ratio of shifts to total warming.

Fig. 2 in the main paper shows the pattern of shifts from regional and global average anomalies (n=45) updated to 2017, showing shifts cooler around 1900, small clusters around 1920, mid 1920s (coinciding with a shift in the Atlantic Meridional Oscillation, AMO), 1936–41, mid to late 1970s (Pacific Decadal Oscillation (PDO) shifts in 1976), 1987–88 (northern hemisphere, NH), 1997–98 (PDO shifts in 1998), 2013–14 (PDO shifts in 2014). Note that some error estimates have been added to the main paper for GMST, TWP and TEP but these are sampling errors only, due to the resampling of a random reference data set.

Ratios of shifts to total warming for the five GMST records in JR2017 range from 0.42 to 0.70 (the 0.42 ratio included a downward shift), but updated to 2018 range from 0.65 to 1.00. Some regions show ratios of >1.00, mostly mid latitudes. This can be compared with the most recent IPCC conclusion as to the human contribution to observed warming. The IPCC concludes that it is extremely likely (95–100%) that human activities caused more than half of the observed increase in

global average surface temperature from 1951 to 2010 (Stocker et al., 2013, p. 60). This conclusion meets the criteria for severe testing, because the alternatives (solar, internal variability, cosmic rays, etc) have been well tested and ruled out (IPCC, 2013).

Shifts total 0.55 °C for the same period. In Table S1 this is compared with three measures of total warming over the same period: the shift and trend process (0.63 °C), a simple trend (0.76 °C; Fig. 1) and the difference between five-year averages centred on 1951 and 2010 (0.64 °C). The proportion of warming allocated to shifts (0.55 °C) ranges from 72% for the simple trend to 86% for the shift and trend process (Table 1). The average rate of change from the internal trends 1951–2010 is 0.015 °C per decade. At that rate, it would take at least 420 years to reproduce the change measured in Table 1. For all five global records of GMST listed above, the average internal trend 1970–2018 would take over 100 years to reproduce 48 years' warming, with NCDC the slowest. Therefore, step-like change dominates over trend-like change over the historical period and trend-like component does not explain the conservative, minimum estimate of forced change.

Table S3: Measurements of temperature change 1951–2010 from Fig. 1, main paper.

	Start	End	Change	Ratio of shifts to total change
Shift & trend	0.19 °C	0.82 °C	0.63 °C	86%
Simple trend	0.02 °C	0.80 °C	0.76 °C	72%
Simple difference	0.16 °C	0.81 °C	0.64 °C	85%

Test 2: The climate model ensemble reproduces the observed pattern of GMST anomalies.

The climate model ensemble reproduces the observed pattern from the 1936 peak in Fig. 2 in the main paper, earlier showing a peak around 1916 and negative shifts associated with the simulated Krakatoa eruption. The correlation between observations and the model ensemble is 0.33 ($p<0.001$). The ensemble historical trend patterns in historical climate are often used to show that models reproduce historical patterns (e.g., Fig 10.7 (Bindoff et al., 2013)) but the same ensemble also produces the historical shift patterns. The presence of downward shifts associated with volcanic forcing indicates that both positive and negative forcing influences the timing and direction of shifts (Reid et al., 2016;Jones and Ricketts, 2021).

Test 3. Testing the rapid and gradual components of modelled GMST anomalies time series against ECS to assess which has the stronger relationship to external forcing.

An updated total of 93 members from the CMIP5 RCP4.5 ensemble have ECS available. Correlations between total shifts, trends and warming 1861–2005 are 0.04, -0.12 and -0.03 respectively. Correlations between of shift magnitude and ECS for on a decadal basis shows negative correlations

in decades with strong volcanic forcing counteract positive forcing later in the record. Correlations 2006–2095 are 0.73, 0.43 and 0.82, for total shifts, trends and warming. When converted into r^2 values (0.53, 0.18, 0.66, respectively), shifts have 2.9 times the influence on ECS compared to internal trends. This is consistent with heat storage and abrupt release from the ocean resulting in rapid positive atmospheric feedback.

Test 4. Regional attribution for three regions in Australia, US and UK.

Regional attribution carried out for SE Australia Central England and Texas, showed an abrupt change from stationary to nonstationary conditions in 1968, 1989 and 1990, respectively. This is counter to the gradual emergence of the signal-to-noise model narrative (Mahlstein et al., 2011;Santer et al., 2011;Hawkins and Sutton, 2012). An earlier nonstationary shift to warmer conditions was detected for Central England temperature in 1911 or 1920, depending on the length of the record used. This may have been due to combination radiative and solar forcing over the NH (Egorova et al., 2018;Hegerl et al., 2018;Wang et al., 2018). Once shifts were identified, internal trends remaining in the data were minimal.

Test 5. Other variables, including temperature extremes, fire weather, rainfall, and local sea level rise show compatible shifts and timing.

A summary of the literature combined with data analyses carried out by the authors listed studies identifying shifts coinciding with the peaks in Fig. 2. We did not conduct a full meta-analysis to identify all shifts, but Reid and Beaugrand (2012) show that shifts surrounding the 1987 regime change are extensive. Beaugrand et al. (2019) have developed protocols for detecting biological shifts in the ocean, that also show synchrony with climate-driven regime shifts, although these protocols do not include attribution.

Test 6. Steps and trends in GMST, 30–60 °N annual, quarterly GMST (2) and quarterly satellite (2) observed time series and four model GMST simulations subject to a variety of tests including heteroscedasticity.

For observations and modelled time series of GMST, simple steps perform better than monotonic change (cubic trend and lowess curve) for goodness of fit (r^2), the residual sum of squares, cumulative) residuals and cumulative residuals squared, White's test for heteroscedasticity, a moving 40-year window regression of the residuals and a moving 40-year window of White's test. A number of additional tests demonstrating that the shifts being detected were not statistical artefacts or the product of system noise were performed by Ricketts (2019). A summary of these relevant is included in the supplementary information.

In conclusion, shifts are clustered around 1921, 1937, 1977 & 1979–80, 1987–88, 1997, 2014–15 and time series are dominated by shifts (rapid change) compared to trends (gradual change, Test 1). In Test 2, the model ensemble showed a better than 1 in 10,000 chance of the similarity between the two not being random. In Test 3, shifts in the model ensemble have 2.9 times the influence of trends. In Test 4, for three regions, warming is step-like and attributed to external forcing. In Test 5, the presence of contemporaneous shifts in some other variables indicate regime shifts in climate are occurring. In Test 6, statistical testing of temperature time series shows that step-like change is a better fit than monotonic change over the period of record.

These results are consistent with a heat storage and release process from the ocean. The presence of shifts to cooler conditions in observations and models suggests that negative forcing may bring cooler water to the ocean surface, cooling the atmosphere. Periods between shifts, such as the so-called hiatus, formed steady-state regimes. This led to a search to understand the physical processes leading to these phenomena.

S1.4. Results and post detection testing

A total of 36 zonal, hemispheric and global records were analysed, 27 for the main paper and 9 extra records covering the extra-tropics and low to mid-latitudes (Table S4). A total of 149 step changes were detected. Of those, 100 are single stationary (67%), 25 single nonstationary (17%), two nonstationary and too short for diagnosis, 19 multiple stationary (13%) and three nonstationary. Of the nonstationary changes, one is 1937 land-ocean 60°S–30°S, a region where issues arise with 1930s–WWII SST data, and the others are 2008 land-ocean and 2009 ocean 90°S–20°S, a large zone that contains multiple changes. Land provides the highest proportion of the single stationary class and ocean the least, just over 50%.

The ANCOVA tests identify few potential false positives. Single nonstationary steps denote the presence of internal trends on one or both sides, where the residuals are autocorrelated. These can be cause by real trends in warming, small shifts or due to the region being influenced be neighbouring areas. Multiple stationary shifts suggest a couple of shift dates close together. Land is the most straightforward with the ocean showing more complex interactions and land-ocean partway between the two, contributing according to the land/ocean ratio of roughly 30:70. The conservative approach to the test means that false negatives, not detecting a shift, is more likely to occur than a false positive.

Table S4: Zonal results for of the MSBV step changes and post detection tests for NCDC mean surface temperature, with the year of the change, the change in °C, classification of change type, ANCOVA results and shift/step ratio of temperature increase.

Surface	Zone	Year of change	Change (°C)	Classification	ANCOVA (p)	Shift/Step ratio
Land	00°N–30°N	1924	0.22	Single, Stationary	0.0002	
Land	00°N–30°N	1979	0.31	Single, Stationary	0.0516	
Land	00°N–30°N	1998	0.60	Single, Stationary	0.0097	0.64
Land	30°S–00°N	1926	0.22	Single, Stationary	0.0012	
Land	30°S–00°N	1957	0.21	Single, Stationary	0.0559	
Land	30°S–00°N	1979	0.42	Single, Stationary	0.0116	
Land	30°S–00°N	2002	0.41	Single, Stationary	0.1143	0.51
Land	20°S–20°N	1903	-0.13	Single, Stationary	0.0000	
Land	20°S–20°N	1926	0.26	Single, Stationary	0.0031	
Land	20°S–20°N	1977	0.39	Single, Stationary	0.0010	
Land	20°S–20°N	1995	0.38	Single, Stationary	0.1827	
Land	20°S–20°N	2009	0.28	Single, Nonstationary	0.0290	0.33
Land	30°N–60°N	1894	0.27	Single, Stationary	0.0124	
Land	30°N–60°N	1921	0.31	Single, Stationary	0.0045	
Land	30°N–60°N	1981	0.44	Single, Stationary	0.0918	
Land	30°N–60°N	1997	0.73	Single, Stationary	0.0512	0.67
Land	60°S–30°S	1938	0.26	Single, Stationary	0.0217	
Land	60°S–30°S	1977	0.43	Single, Stationary	0.0010	
Land	60°S–30°S	2008	0.35	Single, Stationary	0.0671	0.45
Land	60°N–90°N	1920	0.62	Single, Stationary	0.0009	
Land	60°N–90°N	1988	0.80	Single, Stationary	0.0064	
Land	60°N–90°N	2005	0.75	Single, Stationary	0.0466	0.71
Land	00°N–90°N	1894	0.18	Single, Stationary	0.0155	
Land	00°N–90°N	1921	0.30	Single, Stationary	0.0001	
Land	00°N–90°N	1980	0.39	Single, Stationary	0.0013	
Land	00°N–90°N	1997	0.61	Single, Stationary	0.0105	
Land	00°N–90°N	2015	0.45	Multiple, Stationary	0.0019	0.85
Land	90°S–00°N	1926	0.20	Single, Stationary	0.0006	
Land	90°S–00°N	1957	0.19	Single, Stationary	0.0107	
Land	90°S–00°N	1977	0.37	Single, Stationary	0.0061	
Land	90°S–00°N	1997	0.30	Single, Stationary	0.0339	
Land	90°S–00°N	2013	0.27	Multiple, Stationary	0.0780	0.59
Land	90°S–90°N	1894	0.16	Single, Nonstationary	0.0109	
Land	90°S–90°N	1921	0.27	Single, Stationary	0.0002	
Land	90°S–90°N	1977	0.42	Single, Stationary	0.0025	
Land	90°S–90°N	1997	0.56	Single, Stationary	0.0119	
Land	90°S–90°N	2015	0.42	Multiple, Stationary	0.0022	0.73
Land	20°N–90°N	1894	0.22	Single, Stationary	0.0282	
Land	20°N–90°N	1921	0.33	Single, Stationary	0.0005	
Land	20°N–90°N	1981	0.42	Single, Stationary	0.0013	
Land	20°N–90°N	1997	0.67	Single, Stationary	0.0201	
Land	20°N–90°N	2015	0.50	Single, Nonstationary	0.0020	0.85
Land	90°S–20°S	1912	0.26	Single, Stationary	0.0943	
Land	90°S–20°S	1957	0.22	Single, Stationary	0.0928	
Land	90°S–20°S	1977	0.37	Single, Stationary	0.0018	
Land	90°S–20°S	2002	0.29	Single, Stationary	0.0155	
Land	90°S–20°S	2013	0.29	Single, N/A	0.0433	0.92
Land	60°S–60°N	1921	0.31	Single, Stationary	0.0967	
Land	60°S–60°N	1977	0.40	Single, Stationary	0.0238	
Land	60°S–60°N	1997	0.54	Single, Stationary	0.0017	
Land	60°S–60°N	2015	0.37	Multiple, Stationary	0.0039	0.68

Surface	Zone	Year of change	Change (°C)	Classification	ANCOVA (p)	Shift/Step ratio
Land-ocean	00°N–30°N	1926	0.24	Single, Stationary	0.0000	
Land-ocean	00°N–30°N	1979	0.27	Single, Stationary	0.0005	
Land-ocean	00°N–30°N	1997	0.28	Single, Stationary	0.0686	
Land-ocean	00°N–30°N	2014	0.31	Single, Nonstationary	0.0105	0.79
Land-ocean	30°S–00°N	1940	0.22	Single, Stationary	0.0018	
Land-ocean	30°S–00°N	1979	0.39	Single, Stationary	0.0000	
Land-ocean	30°S–00°N	2002	0.26	Single, Stationary	0.0035	0.65
Land-ocean	20°S–20°N	1940	0.21	Single, Stationary	0.0117	
Land-ocean	20°S–20°N	1979	0.35	Single, Stationary	0.0052	
Land-ocean	20°S–20°N	2002	0.29	Single, Stationary	0.0038	0.69
Land-ocean	30°N–60°N	1921	0.30	Single, Stationary	0.0000	
Land-ocean	30°N–60°N	1988	0.36	Single, Stationary	0.0000	
Land-ocean	30°N–60°N	1998	0.41	Multiple, Stationary	0.0015	
Land-ocean	30°N–60°N	2015	0.33	Single, Nonstationary	0.0015	1.03
Land-ocean	60°S–30°S	1938	0.20	Nonstationary	0.0000	
Land-ocean	60°S–30°S	1974	0.37	Multiple, Stationary	0.0000	
Land-ocean	60°S–30°S	2009	0.22	Multiple, Stationary	0.0052	0.71
Land-ocean	60°N–90°N	1920	0.50	Single, Stationary	0.0075	
Land-ocean	60°N–90°N	1988	0.53	Single, Stationary	0.0007	
Land-ocean	60°N–90°N	2002	0.73	Single, Stationary	0.0296	0.74
Land-ocean	00°N–90°N	1925	0.28	Single, Stationary	0.0000	
Land-ocean	00°N–90°N	1987	0.31	Single, Stationary	0.0000	
Land-ocean	00°N–90°N	1997	0.34	Multiple, Stationary	0.0046	
Land-ocean	00°N–90°N	2014	0.34	Single, Nonstationary	0.0003	0.77
Land-ocean	90°S–00°N	1901	-0.17	Single, Stationary	0.0002	
Land-ocean	90°S–00°N	1940	0.24	Single, Stationary	0.0032	
Land-ocean	90°S–00°N	1977	0.34	Single, Stationary	0.0000	
Land-ocean	90°S–00°N	1997	0.16	Single, Stationary	0.3210	
Land-ocean	90°S–00°N	2014	0.17	Single, Nonstationary	0.0130	0.67
Land-ocean	90°S–90°N	1937	0.23	Single, Stationary	0.0000	
Land-ocean	90°S–90°N	1977	0.26	Single, Stationary	0.0000	
Land-ocean	90°S–90°N	1997	0.31	Single, Stationary	0.0119	
Land-ocean	90°S–90°N	2014	0.26	Single, Nonstationary	0.0012	0.71
Land-ocean	20°N–90°N	1921	0.31	Single, Stationary	0.0000	
Land-ocean	20°N–90°N	1988	0.35	Single, Stationary	0.0000	
Land-ocean	20°N–90°N	1998	0.41	Multiple, Stationary	0.0037	
Land-ocean	20°N–90°N	2015	0.37	Single, Nonstationary	0.0218	0.89
Land-ocean	90°S–20°S	1938	0.18	Multiple, Stationary	0.0000	
Land-ocean	90°S–20°S	1972	0.32	Single, Stationary	0.0000	
Land-ocean	90°S–20°S	1997	0.19	Single, Stationary	0.0002	
Land-ocean	90°S–20°S	2009	0.15	Nonstationary	N/A	0.71
Land-ocean	60°S–60°N	1937	0.22	Single, Stationary	0.0001	
Land-ocean	60°S–60°N	1977	0.27	Single, Stationary	0.0000	
Land-ocean	60°S–60°N	1997	0.29	Single, Stationary	0.0079	
Land-ocean	60°S–60°N	2014	0.25	Single, Nonstationary	0.0013	0.74

Surface	Zone	Year of change	Change (°C)	Classification	ANCOVA (p)	Shift/Step ratio
Ocean	00°N–30°N	1936	0.26	Single, Stationary	0.0000	
Ocean	00°N–30°N	1979	0.24	Single, Stationary	0.0188	
Ocean	00°N–30°N	2001	0.19	Multiple, Stationary	0.0480	
Ocean	00°N–30°N	2014	0.30	Single, N/A	0.0007	1.05
Ocean	30°S–00°N	1940	0.20	Single, Stationary	0.0041	
Ocean	30°S–00°N	1979	0.34	Single, Stationary	0.0000	
Ocean	30°S–00°N	2001	0.22	Single, Stationary	0.0019	0.80
Ocean	20°S–20°N	1940	0.23	Single, Stationary	0.0503	
Ocean	20°S–20°N	1979	0.32	Single, Stationary	0.0027	
Ocean	20°S–20°N	2002	0.23	Single, Stationary	0.0018	0.82
Ocean	30°N–60°N	1902	-0.41	Single, Nonstationary	0.0000	
Ocean	30°N–60°N	1915	0.33	Multiple, Stationary	0.0002	
Ocean	30°N–60°N	1930	0.15	Single, Stationary	0.0000	
Ocean	30°N–60°N	1997	0.41	Single, Stationary	0.0000	
Ocean	30°N–60°N	2012	0.26	Single, Nonstationary	0.2781	0.58
Ocean	60°S–30°S	1897	-0.16	Single, Nonstationary	0.0626	
Ocean	60°S–30°S	1938	0.24	Single, Nonstationary	0.0006	
Ocean	60°S–30°S	1974	0.36	Multiple, Stationary	0.0000	
Ocean	60°S–30°S	2010	0.21	Single, Nonstationary	0.0024	0.73
Ocean	60°N–90°N	1926	0.57	Single, Stationary	0.0000	
Ocean	60°N–90°N	1948	-0.23	Single, Stationary	0.0001	
Ocean	60°N–90°N	2000	0.93	Single, Stationary	0.0005	0.48
Ocean	00°N–90°N	1936	0.25	Single, Stationary	0.0000	
Ocean	00°N–90°N	1987	0.19	Single, Stationary	0.0012	
Ocean	00°N–90°N	1997	0.23	Single, Nonstationary	0.0342	
Ocean	00°N–90°N	2014	0.31	Single, Nonstationary	0.0395	0.90
Ocean	90°S–00°N	1901	-0.12	Single, Stationary	0.0000	
Ocean	90°S–00°N	1939	0.24	Single, Stationary	0.0021	
Ocean	90°S–00°N	1977	0.32	Single, Stationary	0.0000	
Ocean	90°S–00°N	1997	0.13	Single, Stationary	0.3300	
Ocean	90°S–00°N	2014	0.15	Single, Nonstationary	0.3300	0.73
Ocean	90°S–90°N	1903	-0.22	Multiple, Stationary	0.0016	
Ocean	90°S–90°N	1914	0.17	Multiple, Stationary	0.0002	
Ocean	90°S–90°N	1937	0.20	Multiple, Stationary	0.0022	
Ocean	90°S–90°N	1977	0.23	Single, Stationary	0.0000	
Ocean	90°S–90°N	1997	0.21	Single, Stationary	0.0393	
Ocean	90°S–90°N	2014	0.21	Single, Nonstationary	0.0070	0.88
Ocean	20°N–90°N	1902	-0.31	Single, Nonstationary	0.0002	
Ocean	20°N–90°N	1915	0.25	Multiple, Stationary	0.0005	
Ocean	20°N–90°N	1930	0.22	Single, Stationary	0.0000	
Ocean	20°N–90°N	1997	0.44	Single, Stationary	0.0000	
Ocean	20°N–90°N	2014	0.32	Single, Nonstationary	0.0013	0.62
Ocean	90°S–20°S	1897	-0.24	Single, Nonstationary	0.0001	
Ocean	90°S–20°S	1938	0.22	Single, Nonstationary	0.0000	
Ocean	90°S–20°S	1972	0.30	Single, Stationary	0.0000	
Ocean	90°S–20°S	1997	0.17	Single, Nonstationary	0.0031	
Ocean	90°S–20°S	2010	0.13	Nonstationary	0.0670	1.00
Ocean	60°S–60°N	1903	-0.23	Multiple, Stationary	0.0020	
Ocean	60°S–60°N	1914	0.18	Single, Stationary	0.0003	
Ocean	60°S–60°N	1939	0.20	Multiple, Stationary	0.0000	
Ocean	60°S–60°N	1977	0.24	Single, Stationary	0.0000	
Ocean	60°S–60°N	1997	0.21	Single, Stationary	0.0463	
Ocean	60°S–60°N	2014	0.22	Single, Nonstationary	0.0044	0.88

Table S4 shows the shift/step ratio ranges between 0.33 for tropical land to 1.05 ocean 0°N–30°N. The results show that land regions have the most straightforward shifts but lower shift/step ratios (average 0.66) than the ocean, which has more complex shifts as shown by their classification, but is also shows higher shift/step ratios (average 0.79). We interpret this as the combination of the land being subject to large-scale atmospheric circulation with some land-surface feedbacks such as ice and snow retreat, and staggered maximum and minimum changes providing mechanisms for some underlying gradual change, and the oceans being subject to more local effects as a product of ocean circulation. The higher shift/step ratios are the result of high negative feedback via ocean surface mixing retaining steady-state conditions.

The ANCOVA results show all detected steps registering as a discontinuity, with 101 $p<0.01$, 28 $p<0.05$ and 13 $p<0.10$ and 5 $p>0.1$ (all recent), with 1 N/A. Of those that exceed $p>0.05$, half are land-based and most are classified as single stationary. None are greater than a one in three chance of being mis-identified.

Overall, these tests show that the risk of false positives is small, in terms of whether the data contains a step change or not. However, shift detection using monthly data shows that some shifts in annual data can either be displaced sightly by an extra hot year for a shift up, or cold year for a shift down. Some of these examples register as multiple stationary. One shift can also register where two of similar magnitude exist either side, the detected shift falling in the middle.

S1.5. Data inhomogeneities

Shifts in SSTs affecting TWP in 1941/42 (upwards) and 1947 (downwards) are considered artefacts. These issues extend across the tropics and southern tropic SSTs (Liu et al., 2015;Folland et al., 2018), whereas further south and north with better shipping coverage, step changes cluster around 1936–38. Changes from NCDCv3 to NCDCv4 moved shifts from earlier to later. Taking the differences for the tropical region between versions, a trend-like adjustment applied in the 1930s moves the 1937 shift to 1940–42, an upward adjustment during WWII that introduces a step change downwards in 1947. For that reason, we consider that the 1937 shift is the real shift (it is maintained at other latitudes and globally). For example, 60°S–30°S monthly data shifts in July 1937. Subsequent post-war cooling is plausible if linked to the phase change in the PDO in 1948, but has not previously registered as a shift in SST. The difference between ERSSTv3 and v4, v5 also partially resemble phase changes in the AMO and PDO, raising the possibility that regressions based on unchanging spatial patterns carrying out adjustments and infills are being affected by reversals of the kind shown in Figure S3. With data adjustment, it is possible that once the first-order issues such as instrument changes are addressed, second-order issues involving adjustments that apply interpolation and

infilling, or longitudinal adjustments, may be influenced by statistical relationships that are assumed to remain constant over time. These relationships may themselves be influenced by changing regimes. Although high quality data sets generally favour better detection of shifts, these analyses suggest that nonlinear variations in climate may need to be factored into second-order adjustments.

S2. Other methods and tests

S2.1. Tracking model

The tracking model, descriptive statistics and manual assessments using the bivariate test were undertaken in Microsoft Excel 2016. The choice was influenced by the exploratory nature of the model and associated tests and the capacity to develop the model in a WYSIWYG environment. The disadvantage of using Excel is that it requires vigilant error-checking of formulae. All methods do, but version control in Excel needs greater care.

The tracking model was built to test the hypothesis that the warm pool acts as a thermostat by maintaining stead-state regimes, undergoing shifts that are propagated outwards and tracking their progress. It was also built to see whether it is possible to track shifts as they evolve, which as yet has not been very successful. Cumulative means of monthly TWP are calculated from a starting point (January 1947). A running six-month mean is also maintained from which the long-term mean is subtracted to produce an anomaly. If that 6-month anomaly is exceeded by a given threshold of 0.2 °C, a flag is raised. The question was if a persistent anomaly emerged (many flags), did that mean a shift was underway?

If a new cumulative mean emerges and persists for 48 months, a shift is called and a new tracking exercise begun. Tracking could not be carried out with TEP because it has high variability, is volatile and does not act as an energy store. The starting point of January 1947 was selected because it comes after WWII anomalies in TWP and precedes the forced period as much as possible. The detailed tracking model results are provided in Section S4 and Table S8.

S2.2. Shifts in autocorrelation

Autocorrelation analyses are conducted with Rodionov's sequential methods for correlation assessment (Rodionov, 2015) regime shift test program v6.2. This tests a time series with its lag-1 pair to determine whether a regime shift in autocorrelation has occurred. Rodionov maintains that time series should be pre-whitened before regime tests (pers. comm.) but this technique shows that the test can detect shifts from red to white noise in time series data.

S2.3. Granger causality testing

Granger causality testing was suggested by a reviewer. The method selected to carry this out is part of Zaiontz' Real Statistics Excel add-on (Release 6.3). http://www.real-statistics.com/free-download/real-statistics-resource-pack/

Annual and monthly temperatures from TEP, TWP, GMST and other regions (29 in total) are tested for correlations and Granger causality. Timeseries have been de-stepped to produce stationary data and tested as observed for both the free and forced periods (1880–1967 and 1968–2018). De-stepping, an alternative to detrending, removes the change in mean during intervals identified by the bivariate test. If the time series is dominated by shifts, de-stepping is the more appropriate action.

Granger causality uses lagged regression. In a stationary timeseries this will test the effect of underlying periodicity, lags affected by phase changes, unit root behaviour and similar. Correlation at time t=0 reflects direct influences such as those due to circulation (monthly, annual) and direct teleconnections (annual). Correlation does not show the direction of flow but the Granger causality data at time t=1,2, … n can show the likely direction at time t=0, indicated by the direction of short-term lags and through lagged correlation. These can be one-way or two-way.

The Granger tests are used to analyse influence for up to lag-24 when possible, and lag-15 for annual data from 1968. For example, t=1 tests lag-1 whereas t=10 test all lags 1 to 10. If lag n+1 has a higher f-test result than lag n then it is considered to have greater influence, implying a causal relationship. For monthly data, the f-test results are preferred to p values because of the large number of samples. Because n is so large, a p-value of 0.01 can be quite weak, so the order of f-test results from large to $p<0.01$ is a better guide. Also, the tests are not measured against the null hypothesis but are conducted to gauge relative influence and how that changes over time. For annual data, p-values above 0.05 represent weak to no influence. Figure 9 shows the p=0.01 and 0.05 curve for f-test values n=139 (the full annual record). P-values are insensitive to n unless n is small.

Testing the observed nonstationary time series disobeys the design rules of the Granger test when assessing it against the test null. Nonstationarity violates the principle of data independence, invalidating p-values. However, our main goal is to compare stationary against nonstationary results and from that infer the non-stationary or forced contribution to change. The stationary results will mainly reflect circulation and teleconnections in steady state.

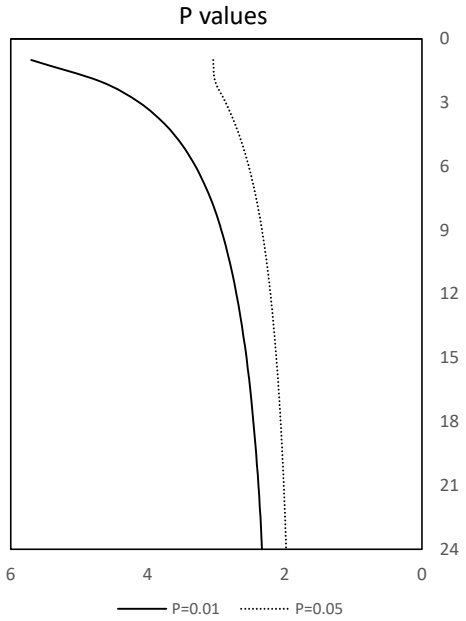

Figure S1: P=0.01 and 0.05 curves for f-test values n=139 (the full annual record 1880–2018).

Sensitivity tests with lagged random data containing steps or trends and with various degrees of autocorrelation were conducted to aid in interpretation. Simple trends and steps produced almost identical results – a high lag-1 value for the f-test statistic, followed by a hyperbolic decrease to low p_{h0} values. Introducing multiple lag effects makes the decrease less hyperbolic. We tested it for n=100 and n=1,000 as a proxy for annual and monthly and it produced a similar pattern of results for both, f-test values increasing for larger n. Testing with observed stationary data and adding steps, trends and autocorrelation showed that lag-2 effects could be produced with TEP and tropical ocean data, but not TWP or land data, which produce lag-1 effects only, unless large amounts of autocorrelation is added.

The testing was accrued out in pairs, for ease of interpretation, but generates a great deal of data for interpretation. Correlations produce 29 x 29 matrices, the Granger tests one less, but the x and y variables are interchanged to assess the direction of influence. For example, to test the influence of TEP on all other variables, 28 results would be produced. When testing all other variables against TEP, another 28 results would be produced. We tested six main pairs: GMST, land ocean, TEP, TWP and tropical ocean (20S–20N), influences to and from. This was done for periods of free and forced climate behaviour, stepped and de-stepped, annual and monthly, adding up to 2,688 pairs in total. We also carried out two-way analyses with the panel and AMO and PDO.

We tested pre- and post-1968 periods representing free and forced behaviour of climate. Monthly data contains 1,668 data points in total, 1,056 to 1968 and 612 from 1968. The de-stepped annual data is stationary using the ADF test and for monthly data is stationary for both the observed and

de-stepped data. The de-stepped annual data was tested for stationarity and whiteness. All de-stepped records are stationary according to the ADF test. Using the Box-Pierce test, 23 of 29 passed for the forced period and 6 of 29 for the forced period, for the Ljung-Box test, 22 of 29 free and 5 out of 29 forced. This is consistent with our testing for GMST, and global land and ocean. The observed data is mainly nonstationary and non-white. The monthly data tested as stationary, but as we show below, is nonstationary with respect to the Granger test, which is why both observed and de-stepped time series are tested.

If shifts are the result of external forcing, removing shifts from timeseries will remove most of this influence. The testing on shifts using ANOVA, ANCOVA and unit root presented above support the interpretation of external influence, as do the probative tests in JR2017. The Granger test treats both steps and trends as a trend, common to most time series analysis methods. We therefore use the de-stepped time series as a control and the observed time series as a measure of forced response, where the difference between the two patterns of change potentially show the main influence on the shift.

Correlations of monthly data at t=0 show how connected regions are on weather timescales. The Granger data shows lag effects and the direction of influence for up to 24 months. Annual data follows similar patterns. Testing TWP, TEP, global, hemispheric and zonal data for land-ocean, land and ocean allows different thermodynamic units to be compared. Lagged correlations show the direction of change. For example, a negative correlation is where cool (warm) temperatures in one region are related to later warm (cool) temperatures in another. Combined Granger and Pearson (correlation) data can show whether temperature flows change direction, strengthen or weaken over time, how much influence TWP and TEP may have on other regions and how other regions affect them.

These interpretations are:

- If an x-y pair shows a large lag-1 effect with a following sharp hyperbolic decrease the influence comes from lag-1 to the current period so is usually preceded by a high correlation. For monthly data, this shows direct circulation. The direction of influence can be tested by comparing opposing pairs' influence on each other, either with the Granger test or lagged correlations.
- If the difference between a nonstationary pair and the observed response shows a large lag-1 effect with a following hyperbolic decrease, the outcome can be interpreted as a simple shift. The direction of forcing can be tested by comparing opposing pairs' influence on each other combined with lagged correlations.

- If the effects decrease according to region size from large to small, the large region is the average of smaller regions that undergo a common change. If a small region shows the largest shift, it has a strong individual influence, especially if the larger region does not share that influence.
- Very low f-test results when the variables have changed by a similar amount over time suggests they are not linked, either physically or through teleconnections. This is evidence they are subject to different physical processes.
- When the stationary data shows strong influences, this may be a sign of continual flux if one-way (e.g., ocean to land) or may be due to variability moving in either direction over time. For example, ENSO effects in a stationary climate and other oscillations will do this.
- In some cases, the stationary time series may exhibit stronger Granger causality than the observed time series. This reflects a relationship that contributes strongly to variability and weakly to change.
- Patterns showing delay and evidence of periodicity (large peaks at lags 2–3 or long trailing influences) are likely to be genuine, even if the f-test and p values are inflated due to nonstationarity, especially with monthly data. Lagged correlations may be needed to test the direction of influence. A lag-2 influence means that the last two time periods contribute to the current value.

S3. Other climate analyses

S3.1. Pacific Decadal Oscillation

Three data sets were downloaded to cross-check data and dates. Four months 1946–48 were missing from the HadSST data set and infilled by averaging the same month from the other two for continuity of analysis. The principal data set used was the ERSST, being the longest.

All were analysed using the bivariate test. Similar inhomogeneities to the other temperature records in the 1930s and 1940s were detected. Monthly data was then used to pinpoint shifts detected on an annual basis. P-values were not considered for monthly changes. The results are shown in Table S5 and inhomogeneities are also noted. The results are discussed in the main paper.

PDO phases with respect to TEP and TWP are shown in Table S6. During negative phases, the difference is 2°C or greater and positive phases <1.9°C (the last period is too short to have a reliable average). The last negative period was 15 years as opposed to the previous two being 29 years in length.

PDO phases are similar to ENSO patterns: positive PDO-El Niño and negative PDO-La Niña (Chen and Wallace, 2015; Newman et al., 2016). Compared to average conditions, positive PDO shows decadal wind anomalies in the west facing east to the cold tongue (i.e., weaker trade winds) with anomalous warming in the cold-tongue and cool anomalies in the north-eastern Pacific and high southern latitudes. The negative phase is cooler in the east but meridional warming is enhanced and the tropical margins are wider (Zhang et al., 2009;Allen and Amaya, 2018).

During its positive phase, the PDO is more restricted to the tropical zone, trade winds are lower and meridional flux is lower (Zhang et al., 2009), leading to more heat being entrained into the warm pool. Because the centre of tropical uplift moves eastward, conditions are also drier and hotter. During the negative phase trade winds are greater, therefore the cold tongue is cooler and meridional transport is enhanced (Zhang et al., 2009). The negative phase of the PDO dissipates more heat out and the cold tongue has greater influence, subject to other influences. The positive phase dissipates heat more upward and gives the warm pool greater influence.

Table S5: Results of bivariate test on three PDO indices performed on annual data then on monthly data.

Ti_0	Year	Change	Period	p value	Month
ERSST (1880–2018)					
4.27	1895	0.42	1880–1925	p>0.25	Jun 1896
9.20	1925	0.79	1880–1947	p<0.05	Aug 1925a
16.52	1942	–1.28	1926–1976	p<0.01	Oct 1942b
7.74	1947	–0.60	1880–1976	p~0.11	Jan 1948
10.98	1976	0.61	1880–2018	p<0.05	Jun 1976
14.70	1998	–1.18	1977–2013	p<0.01	Apr 1998
8.97	2013	1.52	1999–2018	p<0.05	Feb 2014
Mantua (1900–2018)					
6.49	1933	0.48	1900–1947	p<0.01	Jan 1934c
26.81	1947	–0.91	1900–1976	p<0.01	Jan 1948d
25.12	1975	1.28	1948–1988	p<0.01	Jun 1976
12.96	1998	–1.09	1976–2013	p<0.01	Jun 1998
8.88	2013	1.35	1999–2018	p<0.05	Jan 2014
HadSST (1911–2018)					
8.99	1925	0.90	1911–1945	p<0.05	Dec 1925
18.37	1943	–1.19	1926–1976	p<0.01	Mar 1948e
21.68	1976	1.14	1949–1998	p<0.01	Aug 1976
16.83	1998	–1.11	1977–2013	p<0.01	Aug 1998
10.21	2013	1.49	1999–2018	p<0.01	Feb 2014

[a] Inhomogeneities in Apr 1909 and Feb 1934 also
[b] An inhomogeneity noted elsewhere in the paper
[c] As for a
[d] Inhomogeneity in Oct 1942
[e] Inhomogeneity in Aug 1943

S3.2. Atlantic Meridional Oscillation (AMO)

Analysed similarly to the PDO data. The AMO is routinely detrended, but the raw data is also available. This was checked to determine whether the results are any different, but the trend in the AMO is small and both the annual and monthly timing of phase changes remained the same. The largest difference compared to the PDO is that the shifts in the index are identical during two cycles (Table S6) suggesting that forcing is not having a role in that aspect, but only two cycles are inconclusive.

Table S6: AMO phase changes showing the Ti_0 statistic, year before change test period, phase length and month preceding phase change.

Ti_0	Year	Change	Test period	Period length	Month	AMO phase
22.75	1901	-0.17	1856–1925		Apr-02	Positive (–1902)
44.92	1925	0.40	1902–1962	24	Dec-25	Negative (1903–1925)
21.80	1962	-0.17	1926–1994	38	Apr-63	Positive (1926–1962)
39.96	1994	0.40	1963–2018	31	Feb-95	Negative (1963–1994)
	2018			24		Positive (1995–)

Shifts to negative phases have been associated with volcanic forcing (Swingedouw et al., 2017;Birkel et al., 2018) but at high monthly resolution regional shifts precede eruptions for the negative shifts occurring in April 1902 and August 1963. The former preceded the Mt Pelée and Soufrière eruptions that affected the troposphere by one month, and the Oct 1902 Santa Maria eruption that reached the stratosphere by six months (Sato et al., 1993). Earlier shifts were detected in the Atlantic 40°–60° N and Pacific 30–60° S May 1900, and 30° N – 60° N in the Pacific, Atlantic and globally Aug–Nov 1901. By 1903, the shift had registered in the NH and global ocean. The timing suggests cooling was underway before the volcanic eruptions. The mid-latitudes shifted first, followed by TWP and the tropical oceans during 1902–1903. The negative shift in Aug 1963 followed the Agung eruption in March 1963, but was preceded by shifts in the mid to high latitude Atlantic Ocean May–Jun 1962. These shifts were restricted to the Atlantic Ocean.

The positive shift in Dec 1925 was preceded by shifts in SST 0– 30° N in Nov 1923 and high latitude Atlantic Jan 1924, and TWP in Sep 1925, and shows a horseshoe pattern in the Atlantic typical of the AMO positive mode (Ricketts, 2019). The shift in PDO was the only non-Atlantic factor in this sequence. Müller et al. (2015) reproduced the downward shift around 1901 and the following upward shift in a reanalysis model, noting the similarities with the 1995 shift in the same region, showing it to be a robust response.

The timing of the AMO, PDO and regime changes suggests that the two oscillations are at times coupled. In 1902 and 1925, the PDO preceded the AMO, whereas in 1995, the AMO preceded the next shift in TWP and change in phase of the PDO five years later.

S3.3. Autocorrelation

The main results are in the paper and regional results are summarised here. NH SST (0.52) and tropical SST (0.28) do not change over the record, but 0–30° N decreases from 1999 (0.44 to -0.11), 30–60° N increases from 1940 (0.11 to 0.52) and 60–90 N increases from 1919 but drops back from 1947 (0.17 to 0.75 to 0.46). SH SST decreases from 1979 (0.57 to 0.09), with 0–30° S decreasing in 1957 (0.58 to 0.15) and 30–60 S in 1952 (0.68 to 0.33). This indicates the ocean south of 30° N is becoming more prominent in driving change and the higher latitude oceans less so.

NH land autocorrelation decreases in 1971 (0.28 to -0.13), the negative mode indicating short-term oscillations. Tropical land remains constant (0.20), 0–30° N land decreases in 1917 (0.50 to 0.08), 30–60° N in 1906 (0.43 to -0.02) and 60–90° N remains constant (0.00). SH land deceases in 2000 (0.34 to -0.40), 0–30° S and 30–60° S remain constant (0.24, 0.21). The NH data reflects the dissipation of heat polewards, being largely whitened since the early 20th century. The SH data reflects an increase in oscillatory behaviour in the latter part of the record.

S4. Tracking model results in greater detail

This section describes the tracking model results summarised in the main paper. Detailed timing is shown in Table S9 and for the Pacific and Atlantic Ocean basins in Table S10. Some revisions have been made to the results of the MSBV where monthly results indicated that an annual shift was situated roughly midway between two monthly shifts that resolved into two annual shifts, both $p<0.01$, or $p<0.01$ and $p<0.05$. The monthly shifts also indicted that annual shifts can be displaced by a few years due to the way that interannual variability plays out. Based on few revisions in Table S9, the current version of the MSBV is potentially more strict than it needs to be, with some false negatives being recorded.

1968–71: The 0.2°C threshold for TWP was breached from Aug 1968 to Sep 71. For annual data 60°S–30°S land-ocean and ocean shifted in 1969; at monthly scale both shifted in Dec 68. Monthly data for TWP selects May 68 and quarterly data JJA 68 shifting six months before the 60°S–30°S zone. Land 60°S–30°S shows no shift, but Australian SST and south-east Australian min temp shifts in 1969. Sustained warming through the 1969–70 El Niño helped maintain high temperatures in the region and both temperature and rainfall shifted upwards in the Australian region in 1973. Separating out different ocean basins shows that the 1969 shifts occurred both in the Pacific and

Atlantic oceans, indicating a poleward movement of weather systems, consistent with the downward shift of rainfall in south-west WA (Li et al., 2005;Hope et al., 2006).

Tracking the change in real time, the fastest detectability is in the 60°S–30°S ocean, attaining $p<0.05$ with 1971 data and $p<0.01$ with 1973 data. It exceeds $p<0.05$ using 1980–83 data and exceeds $p<0.01$ using 1984–89 data, but using the full historical time series the 1968 shift is eventually dropped in favour of 1979. This is why Fig 1a does not show the 1968 shift but Fig. 2a does.

1976–79: TEP, TWP and the 60°S–30°S zone shifted in 1977 at the annual scale, but at monthly scale the PDO shifted in Jul 76, TEP in Aug 76 and areas of tropical and SH ocean later in 1976. Due to high interannual variability in TEP, the 1977 shift did not emerge from the noise until 1988 at $p<0.05$ and 1993 at $p<0.01$, whereas in 60°S–30°S ocean, it emerged using 1979 and 1981 data, respectively. This shows the benefit of being able to track change in regions of low variability and/or where the shift is largest.

The episode shows two heat shifts. One ocean-driven originating in the E Pacific in mid-1976 and propagating into the SH higher latitudes. The other atmosphere-driven originating in the W Pacific and propagating to the northern hemisphere. The first shift, part of the well document regime shift in the Pacific (Hare and Mantua, 2000;Bond et al., 2003;O'Kane et al., 2014) was large enough to register at hemispheric and global scale.

1986–88: The warm pool exceeded the 0.2°C threshold from Mar 88 to Jan 89. The earliest sign of a potential regime change was registered as 1988 in the 30°N–60°N zone by 1990, passing the $p<0.01$ threshold immediately. Its main impacts were felt in western Europe and parts of north America, coinciding with the 1988 US drought. Using the full record of historical data, NH and global shifts register in 1987.

At monthly scale, global ocean registers a shift in Dec 86 and the NH ocean in Mar 86 and land-ocean Jun 87, followed by land-ocean, land and ocean. Further shifts occurred 30°N–60°N and 60°N–90°N Jan–Apr 88. This shift did not originate in either TEP or TEP, but the timing indicates that the 1987–88 El Niño event was a source of atmospheric warming. The leading indicator is the NH tropical Ocean in Oct 86 at $p<0.1$ annually. This suggests a tropical origin for a regime shift in the shallow ocean, possibly in the tropical Atlantic, although analyses suggest the northern Pacific was involved later (Hare and Mantua, 2000;Tian et al., 2004). Regression analysis also suggests an involvement for both the AMO and Antarctic Oscillation (Reid et al., 2016) and Belilopetsky et al. unpublished.

1995–98: TWP exceeded the 0.2°C threshold from Aug 95 to Feb 97 and again from Aug 98 to Mar 99. This was associated with a chain of shifts ranging from 1997 to 2002 measured at the annual

scale, mostly focusing down to Feb 96 to Apr 98 at monthly timescale, with a couple of exceptions delayed until the 2001 – 02 El Niño. The AMO shifted in Mar 85 and TWP in Apr 95, followed by land-ocean and ocean 60°S–30°S in Feb 96, and land 60°S–30°S in Aug 96. A shift to drier, hotter conditions was identified by the (Bureau of Meteorology, 2006). In the NH, shifts began in Jan 97, registering on NH land and specific zones through to Apr 98.

In tracking terms 60°S–30°S passes the $p<0.05$ threshold in 2001 but does not exceed the $p<0.01$ threshold until 2009. The WP registers the 1995 shift at $p<0.05$ in 1997, but that drops back below until 2002, passing $p<0.01$ in 2003. After the strong La Niña in 1999–2000 sustained warmer conditions were required in order to declare a regime shift rather than a single extreme El Niño. Warmer conditions after 2010 pushed some annual shifts from 97–98 to 2001–02.

Using annual data, the AMO shifted negative to positive in 1995, Mar 95 using monthly data, one month before the WP shifted. The PDO shifted in Jun 98, marking the beginning of the strong La Niña and a negative PDO regime. Based on timing, this suggests a teleconnection between the AMO and warm pool during early 1995, the reverse of the positive to negative shift in the AMO in 1902. The El Niño in 1997–98 was the last of the positive PDO regime.

Late 2000s: This period focuses on a few anomalous shifts during the 2000s. An isolated shift 60°N–90°N land in 2005 is located in Jan 05 and the ocean in Jul 09. Tropical land 20°S–20°N a shift is detected in Nov 2008 which needs more investigation.

A warm pool anomaly of sustained 0.2 °C occurred in Sep 09 and Aug 10–Oct 10. A shift detected in 2010 annually, Dec 09 in land-ocean and ocean 60°S–30°S are associated with shifts in the Australian region (Jones and Ricketts, 2019). This shift to the Australian region preceding a larger Pacific-wide shift could be analogous to 1968, where a shift into the SH mid latitudes preceded the large 1976/77 shift.

2013–15: TWP registers a shift in Dec 12 and exceeded the 0.2°C threshold Sep–Oct 13, Sep 14–Feb 15 and May 16–Mar 17. Shifts are detected in the mid to high NH latitudes in mid to late 2013, at the hemispheric and global scale for ocean and land-ocean in the first half of 2014 and land in the second half. Most heat has gone into the NH, but both hemispheres are affected. The PDO shifted to positive in Mar 14, so follows the WP but precedes a potential shift in TEP by a month. The warm pool therefore led the shift in early 2013 and the mid to high NH latitudes responding that same year. In mid-2014, the PDO shifted with a large El Niño cascading through the tropics and southern hemisphere, as potentially the eastern Pacific warmed as well.

The increase in temperature 2014–2018 over 1997–2013 in the NCDC record is 0.26°C globally, 0.17°C in the SH and 0. 34°C in the NH. Allowing for spatial differences, just over half the warming occurred in SST. In NH latitudinal zones, 00°S–30°N and 30°S–60°N rose by 0.31°C and 60°S–90°N by 0.66°C.

S5. Granger results

Granger analyses and correlations carried out for the 29 climate regions analysed in the project are presented. Correlations are used to assess direct influences and the Granger analyses delayed influences. Analysing free and forced, stationary and nonstationary and monthly and annual data between different thermodynamic units is a complex undertaking because while some results may reflect causal processes, others may reflect a common process with a shared cause and others may be coincidence or statistical artefact. We do not have the space here to do that exhaustively, so restrict ourselves to the main findings that can be independently verified. The full treatment will need to be published elsewhere.

An important part of separating land and ocean into separate units on a zonal basis is to see how the different thermodynamic units with of the climate system interact with each other. The transport of heat between different units as measured by temperature in stable and changing conditions provides the opportunity to identify the nature of those changes. In the following descriptions the stationary data 1880–1967 is nominated as FreeS, nonstationary data Free+, stationary data 1968–2018 ForcedS and nonstationary data Forced+.

S5.1. Ocean

The ocean is a heat sink so whether any other regions contribute additional heat is of interest. During the historical period the oceans cooled then warmed. Between the decade 1880–89 to 1901–10 global SST cooled by 0.24 °C, with most regions similar except for 60–90 °N, which warmed slightly and 30–60 °N, which cooled by 0.42 °C. By 1958–67 global SST had a net warming of 0.10 °C and most other regions a similar amount, except for 60–90 °N, which warmed by 0.37 °C. Global SST from then to 2009–18 warmed by 0.56 °C, TEP by 0.57 °C and TWP by 0.58 °C.

Paired correlations from FreeS with global mean SST range from very low to very high (monthly 0.05 to 0.85; annual 0.18 to 0.92). In ForcedS, this reduces slightly for the monthly data (0.00 to 0.80) and by more for annual data (-0.17 to 0.72). These reductions occur in all 29 regions with annual data and 26 for monthly data. The reduced correlations in the annual data are due to differences between hemispheres becoming more distinct; teleconnections becoming more prominent at the expense of circulation.

For monthly data in FreeS, Granger effects on the ocean are minimal, the largest being TEP (lag-1 f-stat 19.5) and TWP (f-stat 11.5). The influence of TEP is sustained and present in all four cases. TWP is not influential and TEP slightly suppressed in Free+, both play a much larger role In ForcedS (lag-1 TEP 39.3, TWP 33.9) and a lesser but sustained role in Forced+ (lag-5 TEP 10.9, lag-1 TWP 16.5). The only other influences are the central tropical ocean (20 °S – 20 °N), which plays a subordinate role to TEP but follows similar patterns across the four cases; some minor lag-1 land in ForcedS and Forced+ and a major lag-1 input from the high latitude oceans (60–90 °N) during ForcedS.

Annual influences to 1967 are limited to lag-1 influences from southern tropical, SH and central tropical land in FreeS (echoed by tropical and southern tropical land-ocean) and minor lag-1 tropical ocean influence in Free+. From 1968, TEP with a lag-2 peak dominates both ForcedS and Forced+. TEP reaches 10.0 and the central tropical ocean 8.1 at lag-2 in ForcedS and 14.5 and 13.7 respectively, in Forced+. One-third of the regions exceed the nominal $p<0.01$ threshold for lag-2 in Forced+.

The lag-2 peak is not when the shift starts but is the year before the shift, or the launch pad. In stationary conditions the preceding relationship is neutral or negative at lag-2, because it is picking up the ENSO cycle involving El Niño and La Niña. In nonstationary conditions the ENSO cycle is smoothed out by the representation of the average trend. The 1–2 year process revealed by the Granger analysis is consistent with the results of the tracking model.

The lag-1 influences on Forced+ were investigated to see whether central and south tropical land are influenced by TEP at lag-2, which was the case. This shows that these contributions have a flow-on effect, there they have the same origin in TEP, circulating from land back to the ocean. For ForcedS, the stationary case, both positive and negative patterns occur, reflecting the ENSO cycle in the absence of shifts.

S5.2. Land

Paired correlations between stationary data from all regions with global mean LST to 1967 are slightly broader than for SST (monthly 0.01 to 0.98; annual 0.14 to 0.97). After 1967, this barely reduces for the monthly data (0.03 to 0.96), more for annual data (-0.12 to 0.86), mainly in the SH and TEP (0.36 to -0.05). The northern hemisphere is highly correlated with global LST because the large land area and the dominance of short-term variability over land compared to the ocean.

Influence on LST at t=0 is dominated by the NH and 30–60 °N with some input from 60–90 °N land in FreeS and ForcedS, with more involvement of other land regions and oceans in Free+ and Forced+. Monthly lagged inputs (lag-1 tapering) strengthen from FreeS to ForcedS, FreeS+ and Forced+ in that

order. For FreeS, the highest input comes from TEP at f-test 18.3 and the central tropical ocean at 14.6. In Free+ the influence of ocean areas increases with global SST highest at 34.4. For ForcedS, ocean lagged contributions halve and become biased to the SH. For Forced+ both global SST and GMST have an f-test result of 195.6, regional influences in the ocean are widespread, contributions from land-ocean regions do not include those poleward of 30 °N. Land regions have a much smaller contributions, so the main influences are external.

Annual correlations with LST at t=0 have a similar spatial pattern to monthly correlations, but are higher overall, especially ocean regions. Lagged inputs have no influence in FreeS and Free+ except for 60–90 °N with a lag-1 of 10.1 in Free+. ForcedS shows a lag-2 peak for the central tropical ocean and TEP (10.3), with other tropical ocean regions following, and a lag-1 peak for 60–90 °N land and land-ocean (11.8). Forced+ shows both lag-2 and lag-1 effects, with lag-2 <19.2 for TWP and tropical ocean regions and lag-1 <36.5 for global ocean and GMST. The lag-1 response from land regions remains the weakest, with 30–60 °S contributing the most (11.0). The large lag-1 responses from GMST, SST and the NH ocean (>30) shows a widespread influence across most regions with only land-ocean above 30 °N making no contribution.

S5.3. GMST

GMST is the collective measure of ocean, land and all its component regions so provides insight into connectedness and relative contributions to change. Paired correlations between stationary data from all regions with GMST to 1967 are similar to SST (monthly 0.07 to 0.87; annual 0.25 to 0.92). After 1967, this barely reduces for the monthly data (0.00 to 0.86), more for annual data (-0.18 to 0.79), mainly due to reductions in ocean regions while some land regions increase slightly.

The integrative role of GMST is immediately apparent with monthly inputs during FreeS, which range up to lag-1 150.5. Global and NH LST are the largest inputs, but only draw from land N of 30 °N. The tropics including TEP contribute from the ocean (<100.3) and the extratropics do not. Land and ocean regions with no lag-1 have correlations at t=0 of up to 0.38, which exceed the conventional thresholds for statistical significance (p=0.05 0.21, p=0.01 0.27) but lack causation. For Free+ the contributions from land and the tropical ocean regions barely change, from global, NH and SH oceans increase and TEP decreases. The larger lag contributions from global land, global and hemispheric ocean and TWP are sustained over 24 months for FreeS and Free+. For ForcedS, contributions are similar to FreeS but slightly weaker. For Forced+ contributions are also slightly weaker than Free+ at lag-1 but more attenuated over time.

Annual contributions in FreeS and Free+ are minimal, except for a minor lag-1 contribution from global land (7.3) in FreeS and lag-2 TEP (5.2) in Free+. For ForcedS, the largest input is from TEP at

lag-3 (17.4) followed by the tropical ocean at lag-4 (8.1). As the climate is stable, this sequence shows the ENSO cycle in the order of lags 0-pos, 1-pos, 2-neg, 3-neutr, 4-pos, 5-neg. For Forced+ TEP is strongest at lag-2 (25.1) followed by NH, global and tropical oceans, global, NH and high latitude land.

S5.4. TWP

For FreeS correlations between TWP and other regions ranges from -0.06 to 0.18 monthly and -0.03 to 0.39 annually. It decreases slightly in ForcedS to -0.22 to 0.16 monthly and -0.27 to 0.38 annually. In all cases, the lowest correlation is with TEP.

For FreeS, central tropical land and NH and global ocean have a modest lag-1 influence on monthly TWP (<8.3). For Free+, the global ocean and most regions including TEP and except 60–90 °N have some lag-1 influence (<26.5) along with tropical land (16.5). For ForcedS the north tropical, global and south tropical oceans and tropical regions and SH land have the largest lag-1 influence (<14.8) with TEP absent. Forced+ contains the most widespread influences across ocean, land and land-ocean. The ocean involves all regions with the tropics biased north the strongest (<51.4), land with the tropics strongest biased south (<47.5) and land-ocean with an even contribution from both hemispheres (<57.1). TEP plays a small role with lag-1 of 10.8.

Annually in FreeS, influences to TWP are limited to the SH ocean lag-1 (10.9), with a small lag-2 influence from 30–60 °N which translates across to global SST and GMST, and 30 – 60 °S land. TEP is 5.2 at lag-1. For Free+ the pattern is similar but slightly stronger (all regions <17.1). ForcedS is even weaker than FreeS with the tropical oceans and TEP all being below 7.3 lag-1 or weak lag-2, with no input from land except the central tropics (6.1). Forced+ yields widespread influences where proximity to the tropics is the largest distributional effect.

Addressing the influences from TWP, on the FreeS monthly timescale TWP has a strong lag-1 influence on the tropical oceans, especially the central tropics and TEP, but has no influence on land or oceans poleward of 30 °N. When the difference between inputs and outputs are taken into account TWP has a net influence on TEP and the tropical oceans, the latter on a sustained basis. For Free+, the influence from FreeS declines to mainly the central tropical ocean and increases for the 30–60 °S ocean only. Therefore, during this period TWP acts as receiver, but the net forcing in the NH sees TWP influencing the SH ocean to rebalance the two hemispheres.

Monthly ForcedS is a stronger version of FreeS, where the correlation of ocean regions with TWP decreases but their lag-1 influences increase for the tropical regions including TEP. There is no influence on the extratropical ocean or land. For Forced+, influences from TWP become regionalised,

with 60–90 °N being strongly influenced at lag-1 (103.8), a sustained influence on the central tropics for the entire period, a lag-4 influence on the north tropics (12.3), the mid-latitude oceans, a lag-1 influence on the south tropics and global SST (<20.8) and the NH and SH very little. For land, influence on the NH (67.2) and its regions are stronger than for the SH (35.3), except for 30–60 °S (54.3). Land-ocean regions are similarly influenced north of 30° but not at the hemispheric or global scale. Here the net balance for ForcedS is from TWP to the oceans and to the central and southern tropical land-ocean. It is slightly to TWP for land and the rest of the land-ocean regions. This suggests that from 1968, TWP has played a regulatory or stabilising role in the tropics at the sub-annual scale. For Forced+, it is a receiver from most ocean regions and dissipator to the central tropical and mid latitude oceans, consistent with a strengthening of the heat engine and tropical expansion.

For annual influences, in FreeS TWP has a minor lag-1 effect on the global ocean, and north and central tropical ocean (5.0–5.6). In Free+ there is no outward influence. For ForcedS, 0–30 °S ocean, land and land-ocean at lag-1 (11.6–15.2) and the global and SH ocean at lag-2 (6.7 and 5.9). For Forced+ there is a lag-2 influence on the central and south tropical oceans (13.7 and 13.3), global and hemispheric oceans half that; a lag-2 effect on central and southern tropical and SH land (8.4–12.6) and the same regions for land-ocean (7.9–14.9). The 30–60 °S land, ocean and land-ocean has a lag-1 influence (10.8–16.0).

For FreeS and Free+ TWP is a net receiver from all regions, except for 60–90 °N during FreeS. For ForcedS, TWP is a net receiver except for all 30–60 °S regions, and the 60–90 °N ocean. For Forced+ the only exception is the 30–60 °S ocean. This shows that TWP is a net receiver of heat on annual timescales in both stable periods and under change.

S5.5. TEP

For FreeS correlations between TEP and other regions ranges from -0.14 to 0.81 monthly and -0.19 to 0.83 annually. It decreases slightly in ForcedS to -0.22 to 0.80 monthly and -0.27 to 0.75 annually. TEP is mostly highly correlated with the tropics, poorly correlated with the high latitudes and weakly negative with TWP and 30–60 °S.

For FreeS, monthly TEP has lag-2 influences from the central and southern tropical ocean (18.2 and 11.1) and the central tropical land ocean and a lag-1 influence from TWP of 24.1. Most other regions have almost no influence. Free+ is almost identical, except TWP is weaker (14.0). For ForcedS, TWP at lag-1 has the strongest input (48.6) along with central tropical ocean land (50.0). Land influences are lag-1 in the tropics biased south (32.8), and ocean regions (<29.8) omitting the central tropics and 30–60 °N. Forced+ is weaker, with only the central and southern tropics ocean, land-ocean and land and TWP having any influence (<13.4).

Annually for FreeS, TEP receives lag-1 inputs from central and southern tropical land only (11.2 and 8.9). Free+ is weaker, central tropical land reaching a lag-2 of 5.6. For ForcedS, the southern, central and northern tropical and SH oceans have lag-1 inputs of 7.4–21.1, the same regions for land with the central tropics strongest (9.6–13.8) and the same order as for oceans for land-ocean (1.7–17.6). For Forced+, the 30–60 °C oceans and land-ocean (7.7 and 6.4) and 60–90 °N land (6.5) have weak lag-2 inputs.

For TEP's influence on other regions, monthly TEP during FreeS has a strong lag-1 influence on tropical oceans biased north (<57.1), and land and land-oceans biased south (<64.2 and <82.0), with those poleward of 30° being largely unaffected. This influence persists over the period of analysis (24 months). For Free+, the pattern remains the same but lightly weaker for ocean (29.1), land (62.4) and land-ocean (45.5). ForcedS is slightly stronger than p1 (oceans <56.2, land<83.4, land-ocean 120.9) and the tropical bias for all regions is to the south. With the stronger influence, persistence reduces slightly. In Forced+ the pattern remains the same, but slightly weaker than for ForcedS and stronger than Free+ (oceans <39.4, land<58.1, land-ocean <47.8).

Annually for FreeS, TEP's influence is lag-2 except for central tropical land, restricted to the tropical regions (no hemispheric or global influence except for SH land) and symmetrical for all three surfaces (oceans <8.9, land<19.0, land-ocean <13.3). Free+ has a similar pattern but is slightly stronger (oceans <11.7, land<26.4, land-ocean <15.6), land is biased to the tropical south is all lag-2 and land-ocean follows suit. ForcedS TEP influences contain a series of lags; lag-3 to GMST (17.4) and SH land (19.6), lag-2 0–30 °N land-ocean, 0–30 °S land, global land, global ocean (10–19.8) and lag-1 central tropics land and land-ocean, 0–30 °N land and 0–30 °S land-ocean (10.6–21.5). Forced+ is dominated by lag-2 influences with 17 regions being <7.9, land the strongest surface, then land-ocean and ocean.

S5.6. Summary

The net balance of influence is strongest from TEP to other regions on both monthly and annual timescales. Interactions between TWP, TEP and the tropical ocean regions reveal aspects of heat engine behaviour. TWP has a strong lag-1 influence on the central tropical ocean and TEP during stable periods. This strengthens and expands to other ocean regions from 1968. TEP also has strong lag-1 influences to other ocean regions as described above. These have a similar pattern to those from TWP and are stronger during FreeS. During ForcedS, lag-1 influences both strengthen except that TEP's influence in the central tropical ocean decreases where TWP is much stronger. Both have similar patterns on the other tropical regions, hemispheric oceans and global SST, though TEP is slightly stronger in the tropical north.

The central tropical ocean has a strong lag-2 influence on TEP to 1967. From 1968, this changes to a lag-1 influence from the 0–30 °S ocean followed by global SST, showing faster circulation from a wider collection area. TWP shows limited influence from other ocean regions, mainly short-lived lag-1 contributions during ForcedS. TEP and TWP make the strongest contributions to both the central tropical ocean and global SST on a monthly basis during the stable periods FreeS and ForcedS. It is also sustained over the full 24 months and beyond, especially the effect of TEP on the ocean. This level of connectivity is important because these are relatively small regions having a significant influence on tropical and global SST on monthly timescales. The nonstationary cases also indicate that the influence of TEP and TWP are suppressed during periods when shifts are occurring. TWP has less influence in TEP, TEP is less influenced by influences from other regions, TWP's influence on the ocean is suppressed, although this is not the case for land. Normal circulation is potentially being interrupted during such periods.

Annually to 1967, GMST shows minimal external influence. If the period of testing is cut down to 1921–1967, the main two influences on the late 1930s shift are the southern mid-latitude oceans and northern midlatitude land influencing lag-1 global LST (12.7) and global SST (10.0). Interestingly, this again shows N–S symmetry. This indicates that changes during this period were regional.

From 1968, changes become more widespread. TEP and the tropical and NH oceans have a multi-year influence on temperature over a period that matches the ENSO cycle. This is supported by lag correlations between TEP and GMST, positive at lag-0 (not shown), lags-1 and 4, neutral lag-3 and 7, and negative lags 2, 5 and 6 (Fig. 17). For Forced+, TEP leads a strong lag-2 line-up followed by the northern and central tropical, NH and global oceans then global land. In this instance, the lagged correlations between TEP and GMST are positive because of the presence of shifts. TWP does not have a strong direct effect on GMST, but does influence both land and ocean on a strong 2-year lag, so we infer that it has an indirect influence through TEP.

S6. Data sources

S6.1. Global and regional mean surface temperature:

NCDC zonal data version v4.0.1.201801 (Smith et al., 2008;Vose et al., 2012).

Annual and monthly files in ASCII format covering land, ocean, and combined land and ocean were downloaded on 8 – 9 Feb 2019 from ftp://ftp.ncdc.noaa.gov/pub/data/noaaglobaltemp/operational/timeseries/. Each file contains data for one zonal average for land, ocean and combined land and Ocean. Both annual and monthly data were downloaded

The zonal averages used were: 90°S–90°N (Global), 90°S–0°S (°Southern hemisphere), 0°N–90°N (Northern hemisphere), 60°S–30°S, 30°S–0°N, 0°N–30°N, 20°S–20°N, and 60°N–90°N. The zone 90°S–60°S was omitted due to data quality.

Metadata is documented on-line in the file https://www.esrl.noaa.gov/psd/data/gridded/data.noaaglobaltemp.html.

NCDC regional data for SST ERSSTv5 (Huang et al., 2015;Liu et al., 2015;Huang et al., 2016;Huang et al., 2017)

Area averages of the Pacific warm pool and cold tongue regions were produced in February 2019. These areas are delineated following Peyser et al. (2016) (100°W–160°W and 20°S–20°N (TEP) and 120°E–180°E and 20°S–20°N (TWP)).

Metadata is documented on-line in the file https://www.esrl.noaa.gov/psd/data/gridded/data.noaa.ersst.v5.html

Supplementary data has been downloaded from the KNMI climate explorer during 2020 and 2021 when needed. Dates and versions are archived with the data.

S6.2. Pacific Decadal Oscillation (PDO)

Three sets of data were downloaded: ERSST, Mantua and HadSST. These were downloaded from the KNMI climate explorer https://climexp.knmi.nl/selectindex.cgi

ERSSTv5 (Xue et al., 2003;Huang et al., 2017), 1880–2018

Source https://www.ncdc.noaa.gov/cag/global/time-series, https://www.ncdc.noaa.gov/cag/time-series/global/globe/land_ocean/p12/12/1880-2019.csv Extracted Mon Feb 11 2019

PDO Mantua (Mantua et al., 1997;Zhang et al., 1997), 1880–Sep 2018

http://research.jisao.washington.edu/pdo/

Source: UKMO Historical SST data set for 1900-81, Reynold's Optimally Interpolated SST (V1) for January 1982-Dec 2001, OI SST Version 2 (V2) beginning January 2002, Thu Dec 13 2018

PDO HadSST (Morice et al., 2012)

1911–2018 UK Met Office / Hadley Centre

Source: https://www.metoffice.gov.uk/hadobs/hadcrut4/

Extracted Mon Feb 11 MET 2019

S6.3. Atlantic Meridional Oscillation (AMO)

AMO unsmoothed from the Kaplan SST V2 Calculated at NOAA/ESRL/PSD1 (Enfield et al., 2001)

http://www.esrl.noaa.gov/psd/data/timeseries/AMO/, Downloaded February 2019

S6.4. Atlantic Meridional Overturning Circulation (AMOC)

AMOC index HadISST data (Caesar et al., 2018)

http://www.pik-potsdam.de/~caesar/AMOC_slowdown/

http://www.pik-potsdam.de/~caesar/AMOC_slowdown/sg_index_hadisst.txt Downloaded April 2019.

Table S8: Details of selected regime changes produced by the tracking model from 1947 and annual and monthly bivariate tests. All dates register the time of the change. Annual changes p<0.05 are indicated by `, otherwise p<0.01. Where no annual shift is present, a monthly date indicates timing of a minor shift (p≤0.1).

Region	TWP		TEP	PDO	AMO	20°S–20°N			30°S–00°N			00°S–30°N			60°S–30°S			30°N–60°N			60°N–90°N			S Hem			N Hem			Global		
Regime period	T'hold	Shifts	Shifts			L–O*	L	O	L–O	L	O	L–O	L	O	L–O*	L*	O*	L–O	L	O	L–O	L	O	L–O*	L	O	L–O	L	O	L–O	L	O*
1890s				Jul 1896													1897 Nov 1896		1894 May 1893									1894 Jun 1893			1894` Jun 1893	
1900s		1902 May 1902			1902 Apr 1902		1903 Apr 1903				1903` Jan 1903									1902 Nov 1901				1903 Jul 1901		1902 Jun 1901			1902` Apr 1903			1903 Mar 1903
1910s																				1915 Sep 1914				1912 Nov 1911		1912 Dec 1911			1914` Nov 1913			1914 Nov 1913
1921–1930		1921 Nov 1920		Sep 1925	1926 Dec 1925		1926 Oct 1925			1926 Nov 1925		1926 Nov 1925	1924 Nov 1923					1921 Jan 1921	1921 Jan 1921	1930 Sep 1932	1920 Aug 1919	1920 Jul 1919	1926 Jul 1924		1926 Nov 1925		1925 Jul 1925	1921 Jan 1921	1925 Sep 1925		1921 Dec 1920	
1936–1940s		1941 Jan 1941		Jan 1948		1940 Jul 1939		1940 Jul 1939	1940 Dec 1939		1940 Jun 1939			1936 Dec 1935	1938 Aug 1937	1938 May 1938	1938 Aug 1937						1948 Mar 1963	1940 Dec 1939		1939 Mar 1939			1936 Oct 1935	1937 Jul 1936		1937 Jul 1939
1968	Sep 68–Nov 68, Jun 69–Jan 71	May 1968			1964 Aug 1963					1957 Apr 1957					1969 Dec 1968		1969 Dec 1968								1957 Apr 1957							
1976–1979	Sep 78	1979 May 1978	1977 Aug 1976	1976 Jul 1976		1979 Dec 1978	1977 Nov 1976	1979 Jan 1979	1979 Nov 1978	1979 Aug 1979	1979 Oct 1976	1979 Dec 1978	1979 Dec 1978	1979 Sep 1977	1977 Nov 1976	1977 Jan 1977	1977 Nov 1976		1981 May 1980					1977 Nov 1976	1977 Nov 1976	1977 Oct 1976	1977` Sep 1979	1980 Sep 1979		1977 Jun 1979	1977 Aug 1979	1977 Dec 1976
1986–88	Mar 88–Jan 89, Oct 89													Oct 1986				1988 Apr 1988		Jan 1989	1988 Jan 1988	1988 Jan 1988					1987 Jun 1987		1987 Mar 1987			1987 Dec 1986
1995–1998	Aug 95–Feb 97, Aug 98–Mar 99, Jun 01	1995 Apr 1995		1998 Jun 1998	1995 Mar 1995	1997 Jun 1997	1995 Jun 1997	2001 May 1997	2002 May 1997	2002 Mar 2002	2001 Jun 1997	1997 Jun 1997	1998 Jul 1997	2001 May 1997	1996 Feb 1996	1997` Aug 1996	1996 Feb 1996	1998 Feb 1998	1997 Feb 1997	1997 Apr 1998	2002 Jun 2001		2000 Feb 2002	1997 Jun 1997	1997 Jun 1997	1997 May 1997	1997 May 1997	1997 Jan 1997	1997 Jun 2001	1997 Jun 1997	1997 Jun 1997	1997 May 1997
Latter 2000s	Sep 09, Aug 10–Oct 10						2009 Nov 2008								2010 Dec 2009	Sep 2012	2010 Dec 2009					2005 Jan 2005	2011 Jul 2009		Sep 2012						
2013–2015	Sep–Oct 13, Sep 14–Feb 15, May 16–Mar 17	2013 Dec 2012	Oct 2014	2014` Mar 2014		2014` Apr 2014		Apr 2014	2014 Sep 2014	2014` Sep 2014		2014 Apr 2014		2014 May 2014		2013		2015 Jul 2013	2015 Dec 2014	2012 May 2013	Oct 2013			2014 Apr 2014	2013	2014 Mar 2014	2014 Feb 2014	2015 Dec 2014	2014 May 2014	2014 Mar 2014	2015 Dec 2014	2014 Apr 2014

* Results from the MSBV have been recalculated because of anomalies between monthly and annual results, where steps p<0.01 have been missed in the optimisation process or annual data is mistimed due to variability. In both cases, a stable alternative is obtained by using an adjusted interval defined by the monthly results.

` Result p<0.05 added because of interest in the monthly result.

Table S9: Details of selected regime changes produced by the tracking model from 1947 and annual and monthly bivariate tests for the Pacific and Atlantic Basins compared with the whole ocean zone.

Region	TWP		TEP	PDO	AMO	20°S–20°N			30°S–00°N			00°S–30°N			60°S–30°S			30°N–60°N			60°N–90°N			S Hem			N Hem			Global		
Regime period	T'hold	Shifts	Shifts			Pac	Atl	O	Pac	Atl	O	Pac	Atl	O	Pac	Atl	O*	Pac	Atl	O	Pac	Atl	O	Pac	Atl	O	Pac	Atl	O	Pac	Atl	O*
1890s				Jul 1896													1897 Nov 1896															
1900s		1902 May 1902			1902 Apr 1902	1903 Jul 1903	1904 Jul 1902		1903 Mar 1903	1902 Jul 1902	1903` Jan 1903	1903 Mar 1903	1902 Oct 1903		1900 May 1900			1901 Aug 1901	1901 Sep 1901	1902 Nov 1901				1903 May 1903	1902 Mar 1902	1902 Jun 1901	1903 Feb 1903	1902 Nov 1901	1902` Apr 1903	1902 Mar 1903	1902 May 1902	1903 Mar 1903
1910s										1912 Dec 1911			1912 Sep 1914					1914 Aug 1915	1914 Sep 1914	1915 Sep 1914					1915 Oct 1914	1912 Dec 1911	1918 Dec 2017		1914` Nov 1913		1913 Jan 1913	1914 Nov 1913
1921–1930		1921 Nov 1920		Sep 1925	1926 Dec 1925		1926 Nov 1923						1924 Dec 1925						1929 Aug 1929	1930 Sep 1932		1924 Jan 1924	1926 Jul 1924		1926 Jan 1926			1926 Dec 1925	1925 Sep 1925		1932 Feb 1932	
1936–1940s		1941 Jan 1941		Jan 1948		1940 Dec 1939		1940 Jul 1939	1939 Aug 1939	1934 Mar 1934	1940 Jun 1939	1940 Dec 1939	1937 Feb 1937	1936 Dec 1935	1938 Dec 1937	1938 Mar 1938	1938 Aug 1937	1941 Jul 1942					1948	1939 Feb 1939		1939 Mar 1939	1940 Sep 1939		1936 Oct 1935	1939 Jul 1939		1937 Jul 1939
1961–1963					1964 Aug 1963														1961 Apr 1962			1962 Jun 1962	Mar 1963		1964 May 1963			1964 Jul 1964				
1968	Sep 68–Nov 68, Jun 69–Jan 71	May 1968								1972 Jan 1972						1969 Jun 1969	1969 Dec 1968	1968 Aug 1968															
1976–1979	Sep 78	1979 May 1978	1977 Aug 1976	1976 Jul 1976		1979 Oct 1979	1977 Jan 1979	1979 Jan 1979	1979 Mar 1979		1979 Oct 1976		1977	1979 Sep 1977	1979 Dec 1978		1977 Nov 1976							1979 Dec 1978		1977 Oct 1976		1979 Dec 1978		1979 Jan 1979	1979 Feb 1979	1977 Dec 1976
1986–88	Mar 88–Jan 89, Oct 89											1986 Sep 1985	Mar 1987	Oct 1986				1988 Dec 1988	1986 Mar 1987	Jan 1989					1987 Mar 1987		1989 Apr 1989		1987 Mar 1987			1987 Dec 1986
1995–1998	Aug 95–Feb 97, Aug 98–Mar 99, Jun 01	1995 Apr 1995		1998 Jun 1998	1995 Mar 1995		2003 Dec 2002	2001 May 1997	1997 Mar 1997	1998 Oct 1997	2001 Jun 1997		2003 Oct 2002	2001 May 1997			1996 Feb 1996		1997 Feb 1998	1997 Apr 1998		1998 Jul 1997	2000 Feb 2002		1998 Jan 1998	1997 May 1997		1998 Jul 1997	1997 Jun 2001	2001 Mar 2000	1998 Oct 1997	1997 May 1997
Latter 2000s	Sep 09, Aug 10–Oct 10															2009 Dec 2008	2010 Dec 2009					2003 Jun 2002	2011 Jul 2009								
2013–2015	Sep–Oct 13, Sep 14–Feb 15, May 16–Mar 17	2013 Dec 2012	Oct 2014	2014` Mar 2014		2014 Apr 2014		Apr 2014		2016 Dec 2015		2014 May 2014		2014 May 2014	2013 Feb 2013			2012 May 2013	2015 May 2016	2012 May 2013				2015 Apr 2014		2014 Mar 2014	2014 May 2014		2014 May 2014	2015 May 2014	2016 Jan 2016	2014 Apr 2014

Table S10: Correlation matrix for stationary monthly temperature of 29 regions for free (1880–1967) and forced (1968–2018) periods.

Free	TWP	TEP	GMST	NH	SH	Tropics	0-30N	30-60N	60-90N	0-30S	30-60S	Land	NH land	SH land	Tropics lan	0-30N land	30-60N lan	60-90N lan	0-30S land	30-60S lan	Ocean	NH ocean	SH ocean	Tropical oc	0-30N ocea	30-60N oce	60-90N oce	0-30S ocea	30-60S ocean	
TWP		-0.06	0.07	0.06	0.14	0.14	0.16	-0.02	-0.02	0.13	0.03	0.01	-0.01	0.12	0.18	0.07	-0.01	-0.02	0.13	0.01	0.17	0.18	0.11	0.13	0.14	0.02	0.01	0.12	0.02	0.07
TEP	-0.06		0.47	0.33	0.50	0.78	0.67	0.06	-0.02	0.68	-0.08	0.18	0.12	0.29	0.38	0.25	0.08	-0.03	0.31	0.09	0.56	0.56	0.46	0.81	0.75	-0.09	-0.02	0.67	-0.14	0.31
GMST	0.07	0.47		0.87	0.58	0.65	0.52	0.67	0.38	0.68	0.26	0.75	0.70	0.36	0.38	0.29	0.61	0.37	0.36	0.22	0.64	0.59	0.54	0.64	0.58	0.30	0.16	0.64	0.21	0.48
NH	0.06	0.33	0.87		0.29	0.41	0.42	0.85	0.47	0.39	0.16	0.89	0.88	0.20	0.28	0.25	0.81	0.47	0.21	0.06	0.40	0.49	0.26	0.41	0.38	0.35	0.19	0.34	0.09	0.40
SH	0.14	0.50	0.58	0.29		0.66	0.48	0.07	0.09	0.81	0.46	0.22	0.11	0.59	0.47	0.23	0.04	0.08	0.57	0.40	0.84	0.52	0.93	0.67	0.51	0.08	0.10	0.79	0.47	0.42
Tropics	0.14	0.78	0.65	0.41	0.66		0.84	0.04	-0.04	0.90	0.03	0.19	0.10	0.43	0.63	0.44	0.02	-0.05	0.45	0.18	0.74	0.69	0.61	0.99	0.90	-0.01	-0.02	0.86	-0.04	0.41
0-30N	0.16	0.67	0.52	0.42	0.48	0.84		0.02	-0.18	0.66	0.10	0.15	0.08	0.33	0.66	0.68	-0.02	-0.20	0.34	0.10	0.60	0.71	0.43	0.81	0.89	-0.02	-0.09	0.59	-0.02	0.35
30-60N	-0.02	0.06	0.67	0.85	0.07	0.04	0.02		0.34	0.10	0.13	0.88	0.90	0.04	-0.03	0.01	0.95	0.36	0.04	0.00	0.13	0.18	0.06	0.05	-0.01	0.44	0.02	0.07	0.10	0.23
60-90N	-0.02	-0.02	0.38	0.47	0.09	-0.04	-0.18	0.34		0.02	0.08	0.54	0.55	0.04	-0.08	-0.30	0.34	0.98	0.04	0.03	0.13	0.09	0.08	-0.03	-0.08	0.11	0.68	0.02	0.09	0.16
0-30S	0.13	0.68	0.68	0.39	0.81	0.90	0.66	0.10	0.02		0.15	0.24	0.12	0.62	0.56	0.30	0.05	0.01	0.63	0.33	0.75	0.59	0.72	0.89	0.72	0.06	0.01	0.94	0.07	0.43
30-60S	0.03	-0.08	0.26	0.16	0.46	0.03	0.10	0.13	0.08	0.15		0.09	0.05	0.14	0.00	-0.02	0.04	0.08	0.06	0.25	0.36	0.10	0.52	0.05	0.03	0.15	0.03	0.11	0.90	0.15
Land	0.01	0.18	0.75	0.89	0.22	0.19	0.15	0.88	0.54	0.24	0.09		0.98	0.26	0.21	0.17	0.91	0.55	0.26	0.14	0.19	0.19	0.15	0.17	0.10	0.20	0.19	0.17	0.05	0.32
NH land	-0.01	0.12	0.70	0.88	0.11	0.10	0.08	0.90	0.55	0.12	0.05	0.98		0.07	0.11	0.13	0.94	0.57	0.08	0.01	0.13	0.13	0.09	0.09	0.03	0.19	0.19	0.10	0.05	0.27
SH land	0.12	0.29	0.36	0.20	0.59	0.43	0.33	0.04	0.04	0.62	0.14	0.26	0.07		0.54	0.22	0.02	0.04	0.97	0.67	0.34	0.30	0.35	0.38	0.30	0.05	0.07	0.41	0.05	0.29
Tropics lan	0.18	0.38	0.38	0.28	0.47	0.63	0.66	-0.03	-0.08	0.56	0.00	0.21	0.11	0.54		0.68	-0.03	-0.09	0.59	0.14	0.41	0.44	0.36	0.51	0.47	-0.05	0.01	0.46	-0.02	0.29
0-30N land	0.07	0.25	0.29	0.25	0.23	0.44	0.68	0.01	-0.30	0.30	-0.02	0.17	0.13	0.22	0.68		0.01	-0.32	0.23	0.11	0.23	0.28	0.18	0.35	0.39	-0.04	-0.11	0.26	-0.03	0.18
30-60N lan	-0.01	0.08	0.61	0.81	0.04	0.02	-0.02	0.95	0.34	0.05	0.04	0.91	0.94	0.02	-0.03	0.01		0.37	0.03	-0.02	0.05	0.05	0.03	0.03	-0.04	0.20	0.02	0.04	0.04	0.20
60-90N lan	-0.02	-0.03	0.37	0.47	0.08	-0.05	-0.20	0.36	0.98	0.01	0.08	0.55	0.57	0.04	-0.09	-0.32	0.37		0.05	0.03	0.11	0.06	0.08	-0.05	-0.10	0.11	0.58	0.02	0.10	0.15
0-30S land	0.13	0.31	0.36	0.21	0.57	0.45	0.34	0.04	0.04	0.63	0.06	0.26	0.08	0.97	0.59	0.23	0.03	0.05		0.50	0.34	0.31	0.34	0.40	0.31	0.04	0.06	0.43	0.02	0.29
30-60S lan	0.01	0.09	0.22	0.06	0.40	0.18	0.10	0.00	0.03	0.33	0.25	0.14	0.01	0.67	0.14	0.11	-0.02	0.03	0.50		0.19	0.11	0.23	0.17	0.11	0.05	0.08	0.23	0.13	0.16
Ocean	0.17	0.56	0.64	0.40	0.84	0.74	0.60	0.13	0.13	0.75	0.36	0.19	0.13	0.34	0.41	0.23	0.05	0.11	0.34	0.19		0.81	0.85	0.76	0.68	0.28	0.15	0.80	0.36	0.43
NH ocean	0.18	0.56	0.59	0.49	0.52	0.69	0.71	0.18	0.09	0.59	0.10	0.19	0.13	0.30	0.44	0.28	0.05	0.06	0.31	0.11	0.81		0.51	0.71	0.77	0.45	0.15	0.60	0.07	0.38
SH ocean	0.11	0.46	0.54	0.26	0.93	0.61	0.43	0.06	0.08	0.72	0.52	0.15	0.09	0.35	0.36	0.18	0.03	0.08	0.34	0.23	0.85	0.51		0.63	0.47	0.07	0.10	0.80	0.57	0.38
Tropical oc	0.13	0.81	0.64	0.41	0.67	0.99	0.81	0.05	-0.03	0.89	0.05	0.17	0.09	0.38	0.51	0.35	0.03	-0.05	0.40	0.17	0.76	0.71	0.63		0.91	-0.01	-0.02	0.89	-0.03	0.40
0-30N ocea	0.14	0.75	0.58	0.38	0.51	0.90	0.89	-0.01	-0.08	0.72	0.03	0.10	0.03	0.30	0.47	0.39	-0.04	-0.10	0.31	0.11	0.68	0.77	0.47	0.91		-0.01	-0.06	0.69	-0.06	0.35
30-60N oce	0.02	-0.09	0.30	0.35	0.08	-0.01	-0.02	0.44	0.11	0.06	0.15	0.20	0.19	0.05	-0.05	-0.04	0.20	0.11	0.04	0.05	0.28	0.45	0.07	-0.01	-0.01		0.03	0.03	0.10	0.11
60-90N oce	0.01	-0.02	0.16	0.19	0.10	-0.02	-0.09	0.02	0.68	0.01	0.03	0.19	0.19	0.07	0.01	-0.11	0.02	0.58	0.06	0.08	0.15	0.15	0.10	-0.02	-0.06	0.03		0.03	0.08	0.09
0-30S ocea	0.12	0.67	0.64	0.34	0.79	0.86	0.59	0.07	0.02	0.94	0.11	0.17	0.10	0.41	0.46	0.26	0.04	0.02	0.43	0.23	0.80	0.60	0.80	0.89	0.69	0.03	0.03		0.11	0.40
30-60S oce	0.02	-0.14	0.21	0.09	0.47	-0.04	-0.02	0.10	0.09	0.07	0.90	0.05	0.05	0.05	-0.02	-0.03	0.04	0.10	0.02	0.13	0.36	0.07	0.57	-0.03	-0.06	0.10	0.08	0.11		0.12
	0.10	0.33	0.50	0.42	0.44	0.43	0.37	0.26	0.19	0.45	0.18	0.35	0.29	0.32	0.32	0.20	0.23	0.18	0.31	0.19	0.45	0.40	0.40	0.42	0.37	0.14	0.12	0.42	0.15	
Forced	TWP	TEP	GMST	NH	SH	Tropics	0-30N	30-60N	60-90N	0-30S	30-60S	Land	NH land	SH land	Tropics lan	0-30N land	30-60N lan	60-90N lan	0-30S land	30-60S lan	Ocean	NH ocean	SH ocean	Tropical oc	0-30N ocea	30-60N oce	60-90N oce	0-30S ocea	30-60S ocean	
TWP		-0.22	0.14	0.15	0.06	0.06	0.16	0.01	0.05	0.06	0.02	0.11	0.12	0.06	0.08	0.15	0.04	0.05	-0.02	-0.02	0.14	0.03	0.06	0.02	0.13	0.06	0.07	0.07	0.02	0.06
TEP	-0.22		0.38	0.20	0.57	0.80	0.60	-0.04	-0.08	0.70	-0.14	0.06	-0.02	0.42	0.48	0.22	-0.07	-0.04	0.43	0.02	0.69	0.51	0.55	0.63	0.77	-0.09	-0.06	0.73	-0.17	0.28
GMST	0.14	0.38		0.86	0.48	0.57	0.49	0.60	0.38	0.59	0.03	0.82	0.73	0.42	0.35	0.29	0.60	0.39	0.45	0.14	0.64	0.47	0.44	0.35	0.48	0.22	0.05	0.46	0.00	0.42
NH	0.15	0.20	0.86		0.23	0.29	0.28	0.80	0.53	0.26	-0.02	0.88	0.88	0.23	0.20	0.15	0.77	0.54	0.16	0.04	0.44	0.41	0.21	0.24	0.33	0.33	0.12	0.26	-0.03	0.35
SH	0.06	0.57	0.48	0.23		0.72	0.54	-0.06	-0.07	0.81	0.21	0.22	0.07	0.72	0.66	0.34	-0.02	-0.07	0.62	0.27	0.76	0.20	0.94	0.43	0.58	-0.14	-0.09	0.83	0.16	0.36
Tropics	0.06	0.80	0.57	0.29	0.72		0.87	-0.10	-0.07	0.91	-0.19	0.22	0.09	0.58	0.75	0.54	-0.07	-0.07	0.63	0.04	0.78	0.49	0.67	0.60	0.86	-0.13	-0.05	0.81	-0.22	0.37
0-30N	0.16	0.60	0.49	0.28	0.54	0.87		-0.16	-0.17	0.68	-0.11	0.19	0.08	0.45	0.74	0.79	-0.12	-0.19	0.48	0.05	0.68	0.49	0.49	0.51	0.86	-0.14	-0.03	0.58	-0.14	0.32
30-60N	0.01	-0.04	0.60	0.80	-0.06	-0.10	-0.16		0.31	-0.05	0.04	0.77	0.81	-0.01	-0.17	-0.19	0.94	0.35	-0.02	0.00	0.06	0.18	-0.05	0.02	-0.08	0.46	-0.07	-0.03	0.04	0.16
60-90N	0.05	-0.08	0.38	0.53	-0.07	-0.07	-0.17	0.31		-0.04	0.00	0.50	0.53	0.00	-0.10	-0.23	0.29	0.96	-0.04	0.02	0.03	0.11	-0.07	0.01	-0.07	0.07	0.60	-0.04	0.00	0.12
0-30S	0.06	0.70	0.59	0.26	0.81	0.91	0.68	-0.05	-0.04		-0.15	0.27	0.11	0.69	0.66	0.39	-0.01	-0.03	0.74	0.14	0.73	0.35	0.73	0.52	0.69	-0.13	-0.07	0.85	-0.19	0.36
30-60S	0.02	-0.14	0.03	-0.02	0.21	-0.19	-0.11	0.04	0.00	-0.15		0.05	0.03	0.08	-0.08	-0.01	0.07	0.02	-0.01	0.37	0.04	-0.14	0.24	-0.08	-0.09	-0.07	0.05	-0.09	0.97	0.04
Land	0.11	0.06	0.82	0.88	0.22	0.22	0.19	0.77	0.50	0.27	0.05		0.96	0.28	0.19	0.15	0.85	0.53	0.29	0.14	0.20	0.11	0.17	0.11	0.15	0.19	0.07	0.18	0.03	0.31
NH land	0.12	-0.02	0.73	0.88	0.07	0.09	0.08	0.81	0.53	0.11	0.03	0.96		0.09	0.08	0.09	0.90	0.56	0.10	0.02	0.10	0.07	0.07	0.05	0.05	0.20	0.09	0.08	0.03	0.25
SH land	0.06	0.42	0.42	0.23	0.72	0.58	0.45	-0.01	0.00	0.69	0.08	0.28	0.09		0.63	0.30	0.00	-0.01	0.85	0.54	0.49	0.26	0.48	0.36	0.47	0.02	0.02	0.54	-0.06	0.32
Tropics lan	0.08	0.48	0.35	0.20	0.66	0.75	0.74	-0.17	-0.10	0.66	-0.08	0.19	0.08	0.63		0.74	-0.13	-0.08	0.58	0.05	0.51	0.22	0.57	0.41	0.58	-0.20	0.00	0.67	-0.10	0.30
0-30N land	0.15	0.22	0.29	0.15	0.34	0.54	0.79	-0.19	-0.23	0.39	-0.01	0.15	0.09	0.30	0.74		-0.15	-0.23	0.31	0.01	0.34	0.18	0.31	0.25	0.44	-0.17	-0.03	0.38	-0.02	0.19
30-60N lan	0.04	-0.07	0.60	0.77	-0.02	-0.07	-0.12	0.94	0.29	-0.01	0.07	0.85	0.90	0.00	-0.13	-0.15		0.34	0.01	0.00	0.00	0.02	0.00	-0.02	-0.07	0.27	-0.10	-0.01	0.08	0.16
60-90N lan	0.05	-0.04	0.39	0.54	-0.07	-0.07	-0.19	0.35	0.96	-0.03	0.02	0.53	0.56	-0.01	-0.08	-0.23	0.34		-0.05	0.00	0.01	0.06	-0.06	0.01	-0.07	0.03	0.48	0.00	0.03	0.12
0-30S land	-0.02	0.43	0.45	0.16	0.62	0.63	0.48	-0.02	-0.04	0.74	-0.01	0.29	0.10	0.85	0.58	0.31	0.01	-0.05		0.34	0.44	0.37	0.41	0.27	0.45	-0.01	0.07	0.48	-0.10	0.29
30-60S lan	-0.02	0.02	0.14	0.04	0.27	0.04	0.05	0.00	0.02	0.14	0.37	0.14	0.02	0.54	0.05	0.01	0.00	0.00	0.34		0.08	0.04	0.09	0.00	0.06	0.04	0.00	0.02	0.14	0.10
Ocean	0.14	0.69	0.64	0.44	0.76	0.78	0.68	0.06	0.03	0.73	0.04	0.20	0.10	0.49	0.51	0.34	0.00	0.01	0.44	0.08		0.67	0.75	0.57	0.80	0.19	0.04	0.76	0.02	0.39
NH ocean	0.03	0.51	0.47	0.41	0.20	0.49	0.49	0.18	0.11	0.35	-0.14	0.11	0.07	0.26	0.22	0.18	0.02	0.06	0.37	0.04	0.67		0.16	0.41	0.62	0.43	0.27	0.31	-0.17	0.25
SH ocean	0.06	0.55	0.44	0.21	0.94	0.67	0.49	-0.05	-0.07	0.73	0.24	0.17	0.07	0.48	0.57	0.31	0.00	-0.06	0.41	0.09	0.75	0.16		0.41	0.54	-0.17	-0.10	0.84	0.25	0.32
Tropical oc	0.02	0.63	0.35	0.24	0.43	0.60	0.51	0.02	0.01	0.52	-0.08	0.11	0.05	0.36	0.41	0.25	-0.02	0.01	0.27	0.00	0.57	0.41	0.41		0.62	-0.09	0.01	0.56	-0.09	0.25
0-30N ocea	0.13	0.77	0.48	0.33	0.58	0.86	0.86	-0.08	-0.07	0.69	-0.09	0.15	0.05	0.47	0.58	0.44	-0.07	-0.07	0.45	0.06	0.80	0.62	0.54	0.62		-0.05	0.01	0.68	-0.12	0.34
30-60N oce	0.06	-0.09	0.22	0.33	-0.14	-0.13	-0.14	0.46	0.07	-0.13	-0.07	0.19	0.20	0.02	-0.20	-0.17	0.27	0.03	-0.01	0.04	0.19	0.43	-0.17	-0.09	-0.05		0.12	-0.14	-0.09	0.04
60-90N oce	0.07	-0.06	0.05	0.12	-0.09	-0.05	-0.03	-0.07	0.60	-0.07	0.05	0.07	0.09	0.02	0.00	-0.03	-0.10	0.48	0.07	0.00	0.04	0.27	-0.10	0.01	0.01	0.12		-0.06	0.05	0.05
0-30S ocea	0.07	0.73	0.46	0.26	0.83	0.81	0.58	-0.03	-0.04	0.85	-0.09	0.18	0.08	0.54	0.67	0.38	-0.01	0.00	0.48	0.02	0.76	0.31	0.84	0.56	0.68	-0.14	-0.06		-0.11	0.34
30-60S oce	0.02	-0.17	0.00	-0.03	0.16	-0.22	-0.14	0.04	0.00	-0.19	0.97	0.03	0.03	-0.06	-0.10	-0.02	0.08	0.03	-0.10	0.14	0.02	-0.17	0.25	-0.09	-0.12	-0.09	0.05	-0.11		0.01
	0.09	0.30	0.44	0.37	0.38	0.39	0.34	0.18	0.15	0.39	0.07	0.33	0.27	0.34	0.32	0.22	0.19	0.15	0.32	0.13	0.41	0.28	0.34	0.28	0.37	0.07	0.09	0.37	0.04	

Table S11: Correlation matrix for stationary annual temperature of 29 regions for free (1880–1967) and forced (1968–2018) periods.

Free	TWP	TEP	GMST	NH	SH	Tropics	0-30N	30-60N	60-90N	0-30S	30-60S	Land	NH land	SH land	Tropics lan	0-30N land	30-60N lan	60-90N lan	0-30S land	30-60S lan	Ocean	NH ocean	SH ocean	Tropical oc	0-30N ocea	30-60N oce	60-90N oce	0-30S ocea	30-60S ocean	
TWP		-0.03	0.27	0.29	0.37	0.23	0.22	0.08	0.19	0.27	0.20	0.25	0.24	0.16	0.39	0.25	0.14	0.22	0.30	0.04	0.27	0.29	0.34	0.22	0.22	0.10	0.11	0.28	0.20	0.22
TEP	-0.03		0.57	0.52	0.53	0.81	0.77	0.12	0.00	0.72	-0.14	0.38	0.27	0.48	0.53	0.43	0.21	-0.04	0.48	0.31	0.56	0.54	0.43	0.83	0.81	-0.11	0.11	0.71	-0.19	0.38
GMST	0.27	0.57		0.82	0.71	0.85	0.81	0.58	0.30	0.87	0.31	0.49	0.45	0.59	0.52	0.50	0.43	0.25	0.49	0.50	0.92	0.69	0.77	0.85	0.81	0.30	0.25	0.86	0.25	0.57
NH	0.29	0.52	0.82		0.59	0.71	0.67	0.75	0.31	0.72	0.26	0.66	0.63	0.36	0.57	0.55	0.64	0.29	0.54	0.31	0.76	0.83	0.57	0.71	0.69	0.36	0.13	0.72	0.21	0.54
SH	0.37	0.53	0.71	0.59		0.69	0.56	0.31	0.38	0.79	0.53	0.55	0.46	0.52	0.55	0.37	0.29	0.36	0.58	0.55	0.69	0.59	0.91	0.71	0.58	0.21	0.32	0.78	0.46	0.53
Tropics	0.23	0.81	0.85	0.71	0.69		0.93	0.30	0.09	0.94	0.03	0.42	0.32	0.60	0.68	0.60	0.25	0.03	0.56	0.41	0.82	0.66	0.67	0.99	0.94	0.04	0.18	0.92	-0.04	0.52
0-30N	0.22	0.77	0.81	0.67	0.56	0.93		0.25	-0.02	0.81	-0.04	0.34	0.26	0.56	0.66	0.70	0.21	-0.10	0.48	0.30	0.77	0.63	0.55	0.92	0.97	0.04	0.13	0.78	-0.09	0.47
30-60N	0.08	0.12	0.58	0.75	0.31	0.30	0.25		0.28	0.38	0.32	0.66	0.69	0.14	0.15	0.20	0.81	0.29	0.25	0.27	0.50	0.50	0.32	0.30	0.26	0.57	0.06	0.39	0.29	0.36
60-90N	0.19	0.00	0.30	0.31	0.38	0.09	-0.02	0.28		0.18	0.29	0.45	0.50	0.11	0.00	-0.20	0.31	0.97	0.14	0.23	0.18	0.14	0.33	0.10	0.03	0.22	0.74	0.18	0.25	0.24
0-30S	0.27	0.72	0.87	0.72	0.79	0.94	0.81	0.38	0.18		0.19	0.49	0.38	0.67	0.65	0.50	0.29	0.15	0.66	0.54	0.85	0.65	0.78	0.94	0.82	0.13	0.18	0.98	0.11	0.56
30-60S	0.20	-0.14	0.31	0.26	0.53	0.03	-0.04	0.32	0.29	0.19		0.19	0.16	0.02	0.02	-0.05	0.09	0.30	0.11	0.35	0.41	0.38	0.65	0.06	0.00	0.29	0.19	0.23	0.97	0.23
Land	0.25	0.38	0.49	0.66	0.55	0.42	0.34	0.66	0.45	0.49	0.19		0.97	0.49	0.53	0.42	0.84	0.48	0.63	0.44	0.30	0.40	0.40	0.41	0.32	0.14	0.28	0.44	0.15	0.45
NH land	0.24	0.27	0.45	0.63	0.46	0.32	0.26	0.69	0.50	0.38	0.16	0.97		0.37	0.43	0.39	0.89	0.54	0.49	0.35	0.22	0.34	0.34	0.31	0.23	0.16	0.30	0.34	0.14	0.40
SH land	0.16	0.48	0.59	0.36	0.52	0.60	0.56	0.14	0.11	0.67	0.02	0.49	0.37		0.55	0.41	0.26	0.12	0.74	0.71	0.37	0.26	0.47	0.58	0.51	-0.02	0.10	0.53	-0.04	0.38
Tropics lan	0.39	0.53	0.52	0.57	0.55	0.68	0.66	0.15	0.00	0.65	0.02	0.53	0.43	0.55		0.76	0.27	0.00	0.70	0.18	0.46	0.57	0.47	0.64	0.61	-0.12	0.00	0.61	-0.01	0.41
0-30N land	0.25	0.43	0.50	0.55	0.37	0.60	0.70	0.20	-0.20	0.50	-0.05	0.42	0.39	0.41	0.76		0.27	-0.23	0.48	0.16	0.40	0.41	0.33	0.56	0.56	-0.07	-0.03	0.47	-0.08	0.32
30-60N lan	0.14	0.21	0.43	0.64	0.29	0.25	0.21	0.81	0.31	0.29	0.09	0.84	0.89	0.26	0.27	0.27		0.34	0.35	0.27	0.22	0.33	0.20	0.25	0.19	0.20	0.09	0.25	0.08	0.27
60-90N lan	0.22	-0.04	0.25	0.29	0.36	0.03	-0.10	0.29	0.97	0.15	0.30	0.48	0.54	0.12	0.00	-0.23	0.34		0.18	0.23	0.11	0.12	0.30	0.05	-0.04	0.24	0.59	0.14	0.26	0.22
0-30S land	0.30	0.48	0.49	0.54	0.58	0.56	0.48	0.25	0.14	0.66	0.11	0.63	0.49	0.74	0.70	0.48	0.35	0.18		0.47	0.38	0.51	0.48	0.55	0.47	0.04	0.04	0.57	0.06	0.42
30-60S lan	0.04	0.31	0.50	0.31	0.55	0.41	0.30	0.27	0.23	0.54	0.35	0.44	0.35	0.71	0.18	0.16	0.27	0.23	0.47		0.37	0.25	0.57	0.43	0.29	0.16	0.24	0.48	0.23	0.35
Ocean	0.27	0.56	0.92	0.76	0.69	0.82	0.77	0.50	0.18	0.85	0.41	0.30	0.22	0.37	0.46	0.40	0.22	0.11	0.38	0.37		0.75	0.78	0.83	0.82	0.33	0.18	0.89	0.37	0.52
NH ocean	0.29	0.54	0.69	0.83	0.59	0.66	0.63	0.50	0.14	0.65	0.38	0.40	0.34	0.26	0.57	0.41	0.33	0.12	0.51	0.25	0.75		0.64	0.69	0.70	0.33	0.02	0.69	0.34	0.47
SH ocean	0.34	0.43	0.77	0.57	0.91	0.67	0.55	0.32	0.33	0.78	0.65	0.40	0.34	0.47	0.47	0.33	0.20	0.30	0.48	0.57	0.78	0.64		0.69	0.56	0.22	0.28	0.80	0.58	0.52
Tropical oc	0.22	0.83	0.85	0.71	0.71	0.99	0.92	0.30	0.10	0.94	0.06	0.41	0.31	0.58	0.64	0.56	0.25	0.05	0.55	0.43	0.83	0.69	0.69		0.94	0.05	0.18	0.93	-0.02	0.53
0-30N ocea	0.22	0.81	0.81	0.69	0.58	0.94	0.97	0.26	0.03	0.82	0.00	0.32	0.23	0.51	0.61	0.56	0.19	-0.04	0.47	0.29	0.82	0.70	0.56	0.94		0.07	0.15	0.82	-0.05	0.47
30-60N oce	0.10	-0.11	0.30	0.36	0.21	0.04	0.04	0.57	0.22	0.13	0.29	0.14	0.16	-0.02	-0.12	-0.07	0.20	0.24	0.04	0.16	0.33	0.33	0.22	0.05	0.07		0.03	0.16	0.25	0.15
60-90N oce	0.11	0.11	0.25	0.13	0.32	0.18	0.13	0.06	0.74	0.18	0.19	0.28	0.30	0.10	0.00	-0.03	0.09	0.59	0.04	0.24	0.18	0.02	0.28	0.18	0.15	0.03		0.17	0.14	0.18
0-30S ocea	0.28	0.71	0.86	0.72	0.78	0.92	0.78	0.39	0.18	0.98	0.23	0.44	0.34	0.53	0.61	0.47	0.25	0.14	0.57	0.48	0.89	0.69	0.80	0.93	0.82	0.16	0.17		0.17	0.55
30-60S oce	0.20	-0.19	0.25	0.21	0.46	-0.04	-0.09	0.29	0.25	0.11	0.97	0.15	0.14	-0.04	-0.01	-0.08	0.08	0.26	0.06	0.23	0.37	0.34	0.58	-0.02	-0.05	0.25	0.14	0.17		0.18
	0.21	0.41	0.59	0.57	0.55	0.54	0.50	0.40	0.27	0.60	0.26	0.46	0.43	0.40	0.42	0.35	0.35	0.25	0.44	0.38	0.54	0.49	0.53	0.54	0.52	0.19	0.22	0.59	0.21	
Forced	TWP	TEP	GMST	NH	SH	Tropics	0-30N	30-60N	60-90N	0-30S	30-60S	Land	NH land	SH land	Tropics lan	0-30N land	30-60N lan	60-90N lan	0-30S land	30-60S lan	Ocean	NH ocean	SH ocean	Tropical oc	0-30N ocea	30-60N oce	60-90N oce	0-30S ocea	30-60S ocean	
TWP		-0.27	0.35	0.31	0.16	0.15	0.31	-0.02	0.18	0.14	-0.05	0.38	0.19	0.05	0.20	0.28	0.10	0.15	0.06	0.08	0.20	-0.05	0.12	-0.02	0.05	0.01	0.23	0.03	-0.07	0.12
TEP	-0.27		0.30	0.10	0.47	0.73	0.58	-0.12	-0.21	0.50	-0.15	-0.05	-0.06	0.38	0.54	0.40	-0.24	-0.22	0.40	0.07	0.59	0.41	0.46	0.75	0.69	-0.05	-0.10	0.58	-0.18	0.23
GMST	0.35	0.30		0.79	0.66	0.66	0.66	0.37	0.25	0.43	-0.15	0.62	0.49	0.50	0.59	0.50	0.39	0.26	0.37	0.29	0.72	0.37	0.60	0.42	0.46	0.12	0.15	0.38	-0.18	0.41
NH	0.31	0.10	0.79		0.10	0.36	0.46	0.62	0.46	0.13	-0.20	0.58	0.51	0.02	0.18	0.25	0.65	0.49	0.12	0.10	0.45	0.52	0.04	0.17	0.30	0.24	0.22	0.06	-0.21	0.28
SH	0.16	0.47	0.66	0.10		0.68	0.55	-0.20	-0.22	0.59	0.00	0.29	0.13	0.76	0.76	0.52	-0.17	-0.21	0.46	0.35	0.66	-0.02	0.98	0.50	0.38	-0.16	-0.16	0.57	-0.05	0.30
Tropics	0.15	0.73	0.66	0.36	0.68		0.92	-0.06	-0.11	0.76	-0.33	0.40	0.26	0.56	0.72	0.75	-0.09	-0.12	0.64	0.13	0.70	0.37	0.63	0.83	0.84	-0.04	0.00	0.77	-0.38	0.38
0-30N	0.31	0.58	0.66	0.46	0.55	0.92		-0.04	-0.06	0.62	-0.22	0.45	0.31	0.46	0.61	0.81	-0.08	-0.09	0.54	0.18	0.68	0.41	0.49	0.74	0.87	0.07	0.12	0.60	-0.28	0.38
30-60N	-0.02	-0.12	0.37	0.62	-0.20	-0.06	-0.04		0.40	-0.10	0.01	0.53	0.69	-0.06	-0.10	-0.07	0.86	0.44	0.05	0.08	0.12	0.40	-0.24	-0.03	0.03	0.46	0.13	-0.09	0.03	0.15
60-90N	0.18	-0.21	0.25	0.46	-0.22	-0.11	-0.06	0.40		-0.03	-0.03	0.24	0.38	-0.15	-0.03	0.05	0.43	0.98	0.05	-0.27	-0.03	0.16	-0.23	-0.01	-0.05	0.10	0.73	-0.02	-0.01	0.11
0-30S	0.14	0.50	0.43	0.13	0.59	0.76	0.62	-0.10	-0.03		-0.24	0.35	0.16	0.66	0.68	0.66	-0.03	-0.05	0.88	0.02	0.46	0.25	0.56	0.86	0.61	-0.16	0.05	0.95	-0.28	0.34
30-60S	-0.05	-0.15	-0.15	-0.20	0.00	-0.33	-0.22	0.01	-0.03	-0.24		-0.09	0.02	0.02	-0.17	-0.05	-0.07	-0.05	-0.08	0.35	-0.11	-0.14	0.03	-0.16	-0.19	0.28	0.04	-0.24	0.97	-0.04
Land	0.38	-0.05	0.62	0.58	0.29	0.40	0.45	0.53	0.24	0.35	-0.09		0.86	0.28	0.30	0.41	0.60	0.28	0.39	0.16	0.38	0.16	0.21	0.22	0.27	0.31	0.05	0.25	-0.12	0.31
NH land	0.19	-0.06	0.49	0.51	0.13	0.26	0.31	0.69	0.38	0.16	0.02	0.86		0.23	0.15	0.37	0.63	0.42	0.33	0.06	0.22	0.21	0.07	0.20	0.30	0.51	0.16	0.18	0.02	0.29
SH land	0.05	0.38	0.50	0.02	0.76	0.56	0.46	-0.06	-0.15	0.66	0.02	0.28	0.23		0.72	0.56	-0.06	-0.14	0.75	0.31	0.40	0.14	0.70	0.57	0.51	-0.03	-0.09	0.64	-0.04	0.31
Tropics lan	0.20	0.54	0.59	0.18	0.76	0.72	0.61	-0.10	-0.03	0.68	-0.17	0.30	0.15	0.72		0.67	-0.06	-0.01	0.61	0.08	0.55	0.14	0.70	0.64	0.53	-0.15	-0.03	0.65	-0.17	0.33
0-30N land	0.28	0.40	0.50	0.25	0.52	0.75	0.81	-0.07	0.05	0.66	-0.05	0.41	0.37	0.56	0.67		-0.13	0.01	0.68	0.06	0.50	0.34	0.48	0.72	0.73	0.08	0.22	0.67	-0.12	0.37
30-60N lan	0.10	-0.24	0.39	0.65	-0.17	-0.09	-0.08	0.86	0.43	-0.03	-0.07	0.60	0.63	-0.06	-0.06	-0.13		0.48	0.02	0.01	0.00	0.20	-0.21	-0.11	-0.09	0.26	0.10	-0.09	-0.03	0.10
60-90N lan	0.15	-0.22	0.26	0.49	-0.21	-0.12	-0.09	0.44	0.98	-0.05	-0.05	0.28	0.42	-0.14	-0.01	0.01	0.48		0.05	-0.26	-0.07	0.10	-0.23	-0.05	-0.09	0.10	0.57	-0.06	-0.02	0.10
0-30S land	0.06	0.40	0.37	0.12	0.46	0.64	0.54	0.05	0.05	0.88	-0.08	0.39	0.33	0.75	0.61	0.68	0.02	0.05		0.07	0.35	0.31	0.40	0.81	0.62	0.05	0.07	0.84	-0.12	0.35
30-60S lan	0.08	0.07	0.29	0.10	0.35	0.13	0.18	0.08	-0.27	0.02	0.35	0.16	0.06	0.31	0.08	0.06	0.01	-0.26	0.07		0.31	0.09	0.29	0.03	0.10	0.07	-0.19	-0.02	0.23	0.10
Ocean	0.20	0.59	0.72	0.45	0.66	0.70	0.68	0.12	-0.03	0.46	-0.11	0.38	0.22	0.40	0.55	0.50	0.00	-0.07	0.35	0.31		0.58	0.63	0.57	0.51	0.06	0.13	0.46	-0.17	0.35
NH ocean	-0.05	0.41	0.37	0.52	-0.02	0.37	0.41	0.40	0.16	0.25	-0.14	0.16	0.21	0.14	0.14	0.34	0.20	0.10	0.31	0.09	0.58		-0.05	0.48	0.57	0.25	0.29	0.29	-0.17	0.24
SH ocean	0.12	0.46	0.60	0.04	0.98	0.63	0.49	-0.24	-0.23	0.56	0.03	0.21	0.07	0.70	0.70	0.48	-0.21	-0.23	0.40	0.29	0.63	-0.05		0.48	0.34	-0.19	-0.13	0.58	0.00	0.27
Tropical oc	-0.02	0.75	0.42	0.17	0.50	0.83	0.74	-0.03	-0.01	0.86	-0.16	0.22	0.20	0.57	0.64	0.72	-0.11	-0.05	0.81	0.03	0.57	0.48	0.48		0.85	0.01	0.13	0.91	-0.19	0.37
0-30N ocea	0.05	0.69	0.46	0.30	0.38	0.84	0.87	0.03	-0.05	0.61	-0.19	0.27	0.30	0.51	0.53	0.73	-0.09	-0.09	0.62	0.10	0.51	0.57	0.34	0.85		0.16	0.15	0.67	-0.23	0.35
30-60N oce	0.01	-0.05	0.12	0.24	-0.16	-0.04	0.07	0.46	0.10	-0.16	0.28	0.31	0.51	-0.03	-0.15	0.08	0.26	0.10	0.05	0.07	0.06	0.25	-0.19	0.01	0.16		0.09	-0.13	0.24	0.09
60-90N oce	0.23	-0.10	0.15	0.22	-0.16	0.00	0.12	0.13	0.73	0.05	0.04	0.05	0.16	-0.09	-0.03	0.22	0.10	0.57	0.07	-0.19	0.13	0.29	-0.13	0.13	0.15	0.09		0.11	0.03	0.11
0-30S ocea	0.03	0.58	0.38	0.06	0.57	0.77	0.60	-0.09	-0.02	0.95	-0.24	0.25	0.18	0.64	0.65	0.67	-0.09	-0.06	0.84	-0.02	0.46	0.29	0.58	0.91	0.67	-0.13	0.11		-0.26	0.33
30-60S oce	-0.07	-0.18	-0.18	-0.21	-0.05	-0.38	-0.28	0.03	-0.01	-0.28	0.97	-0.12	0.02	-0.04	-0.17	-0.12	-0.03	-0.02	-0.12	0.23	-0.17	-0.17	0.00	-0.19	-0.23	0.24	0.03	-0.26		-0.06
	0.13	0.27	0.42	0.31	0.32	0.40	0.42	0.17	0.14	0.39	0.01	0.31	0.32	0.33	0.35	0.41	0.14	0.13	0.39	0.12	0.37	0.29	0.29	0.39	0.40	0.13	0.14	0.39	-0.02	

Plate 1: To Land Monthly (top) and Annual (bottom)

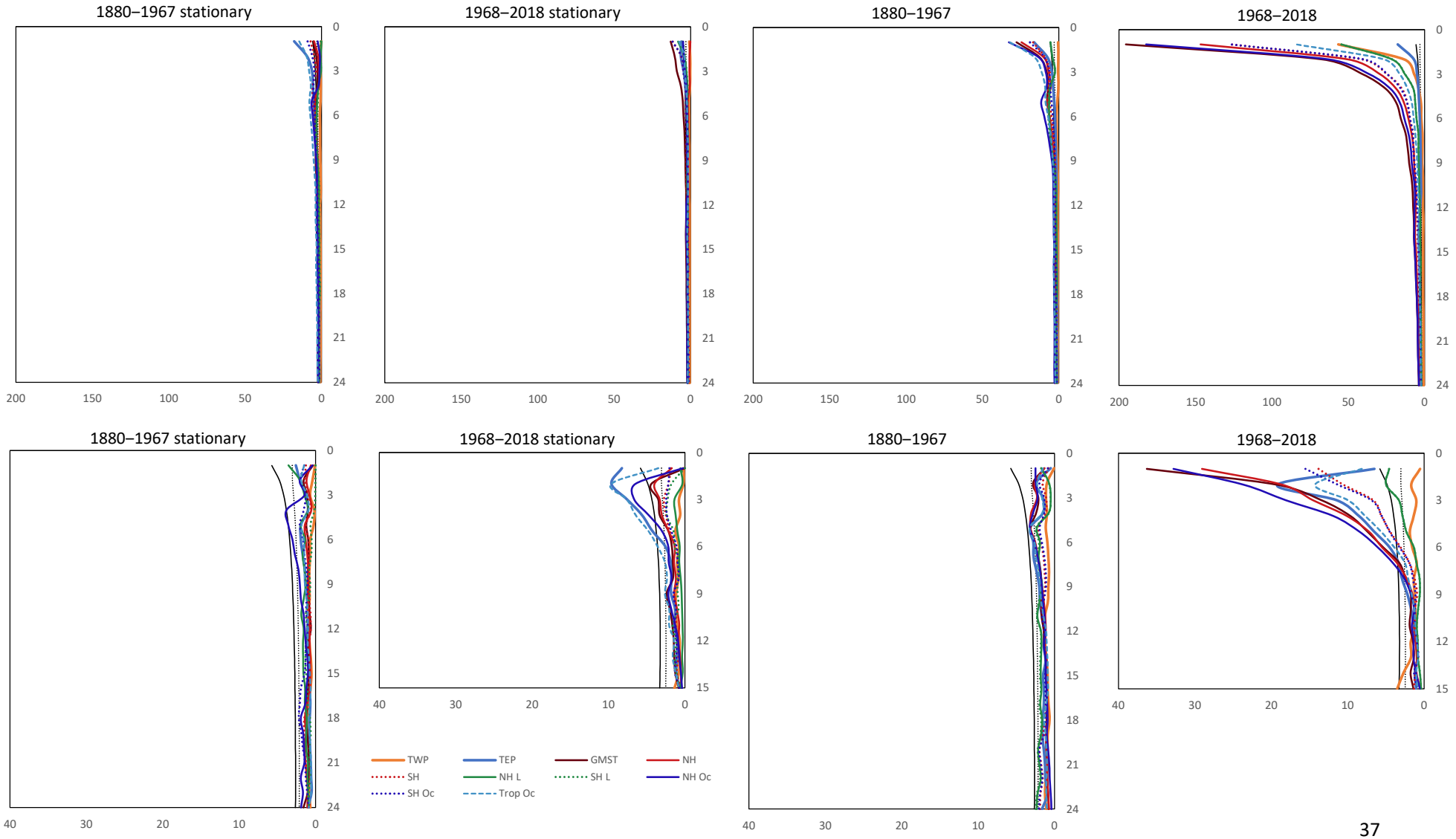

Plate 2: From Land Monthly (top) and Annual (bottom)

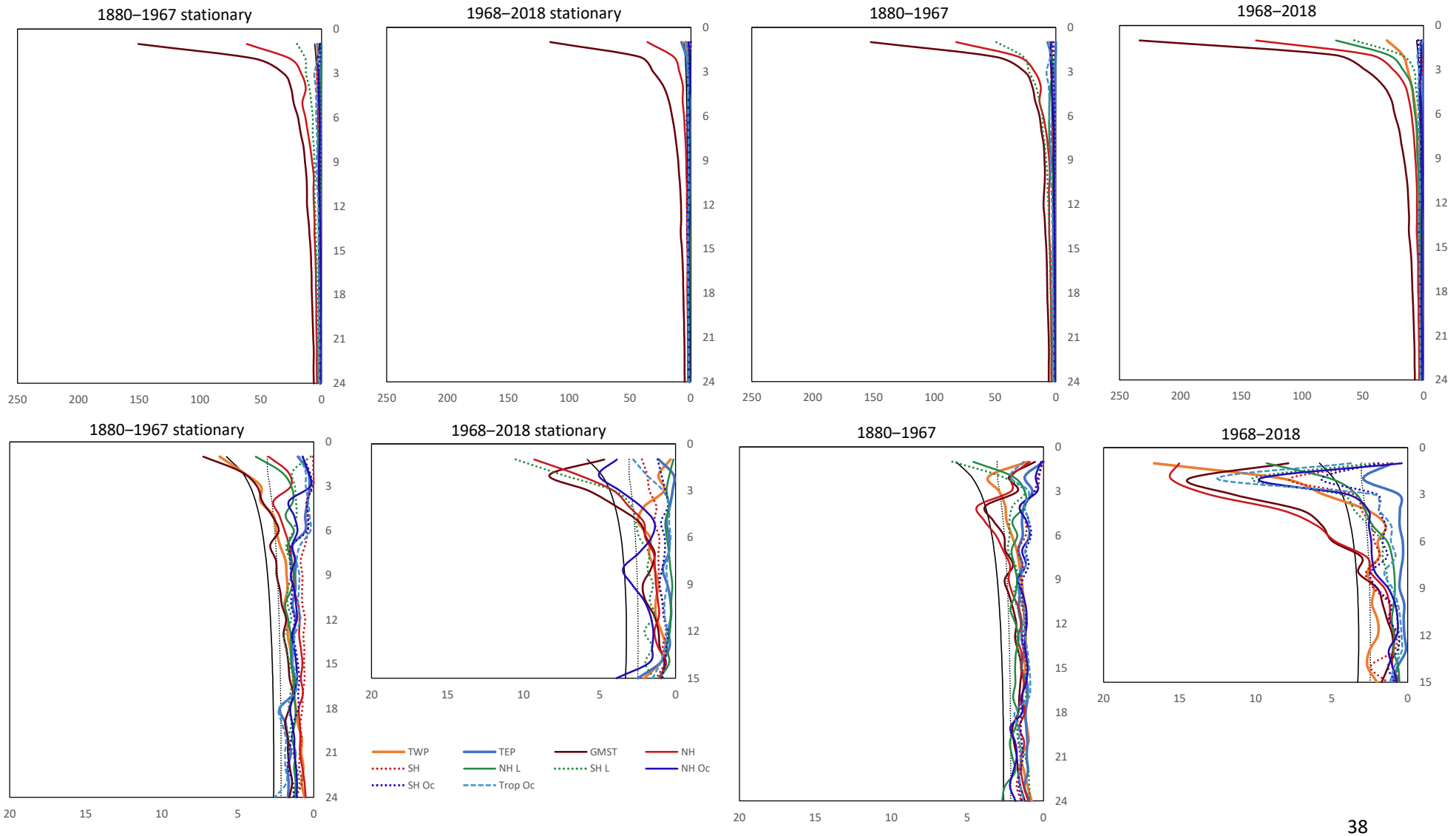

Plate 3: To Ocean Monthly (top) and Annual (bottom)

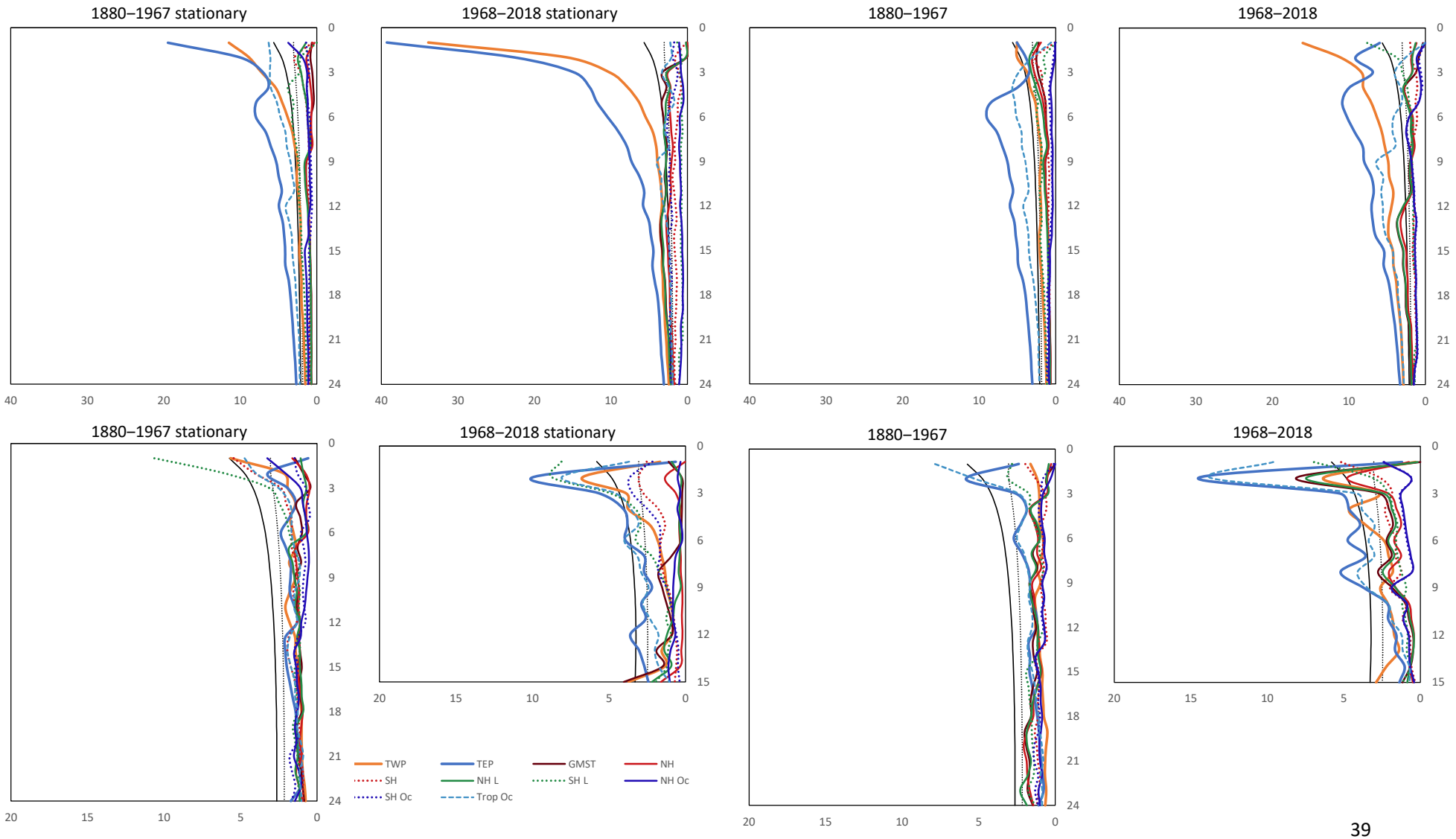

Plate 4: From Ocean Monthly (top) and Annual (bottom)

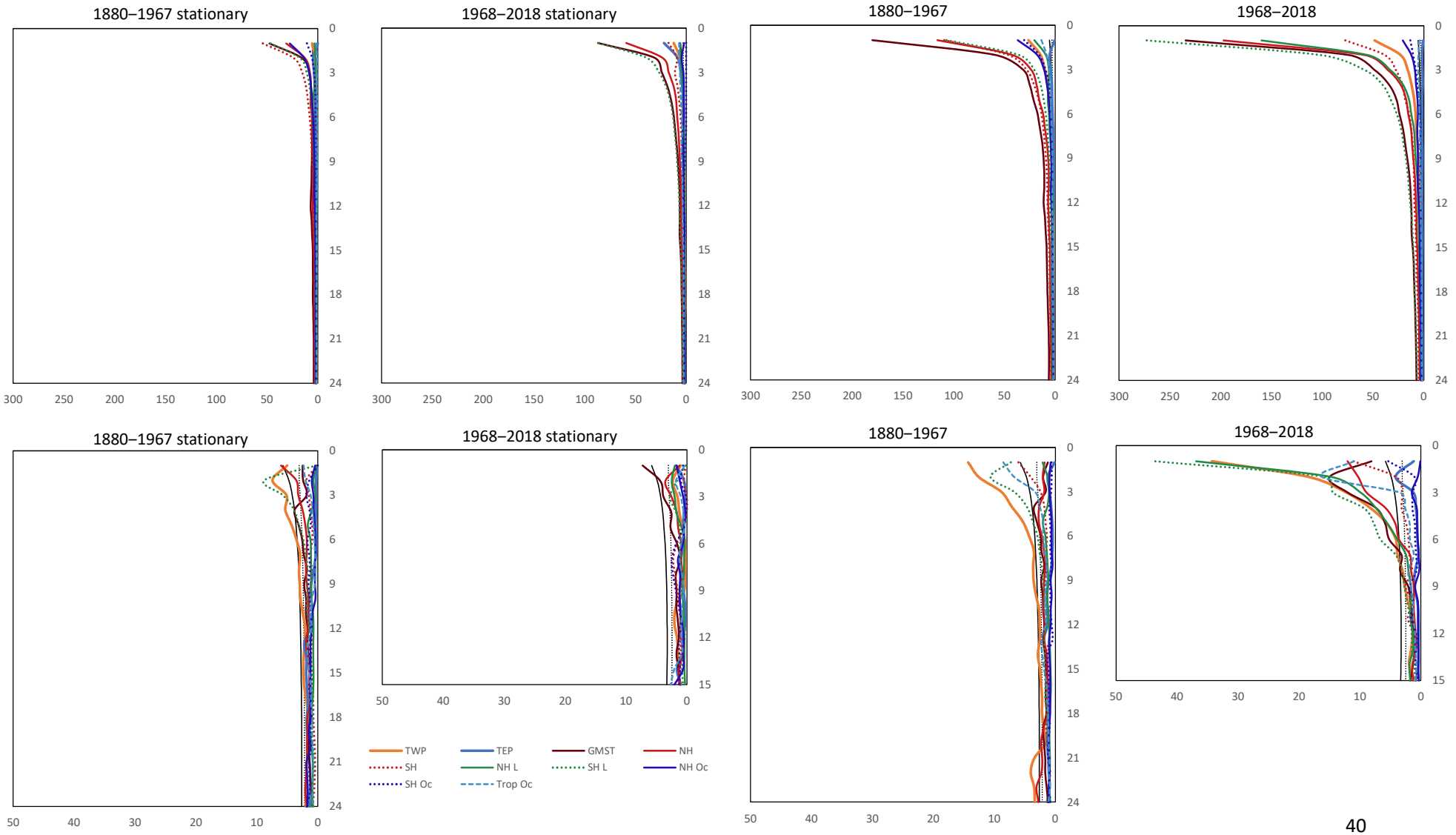

Plate 5: To GMST Monthly (top) and Annual (bottom)

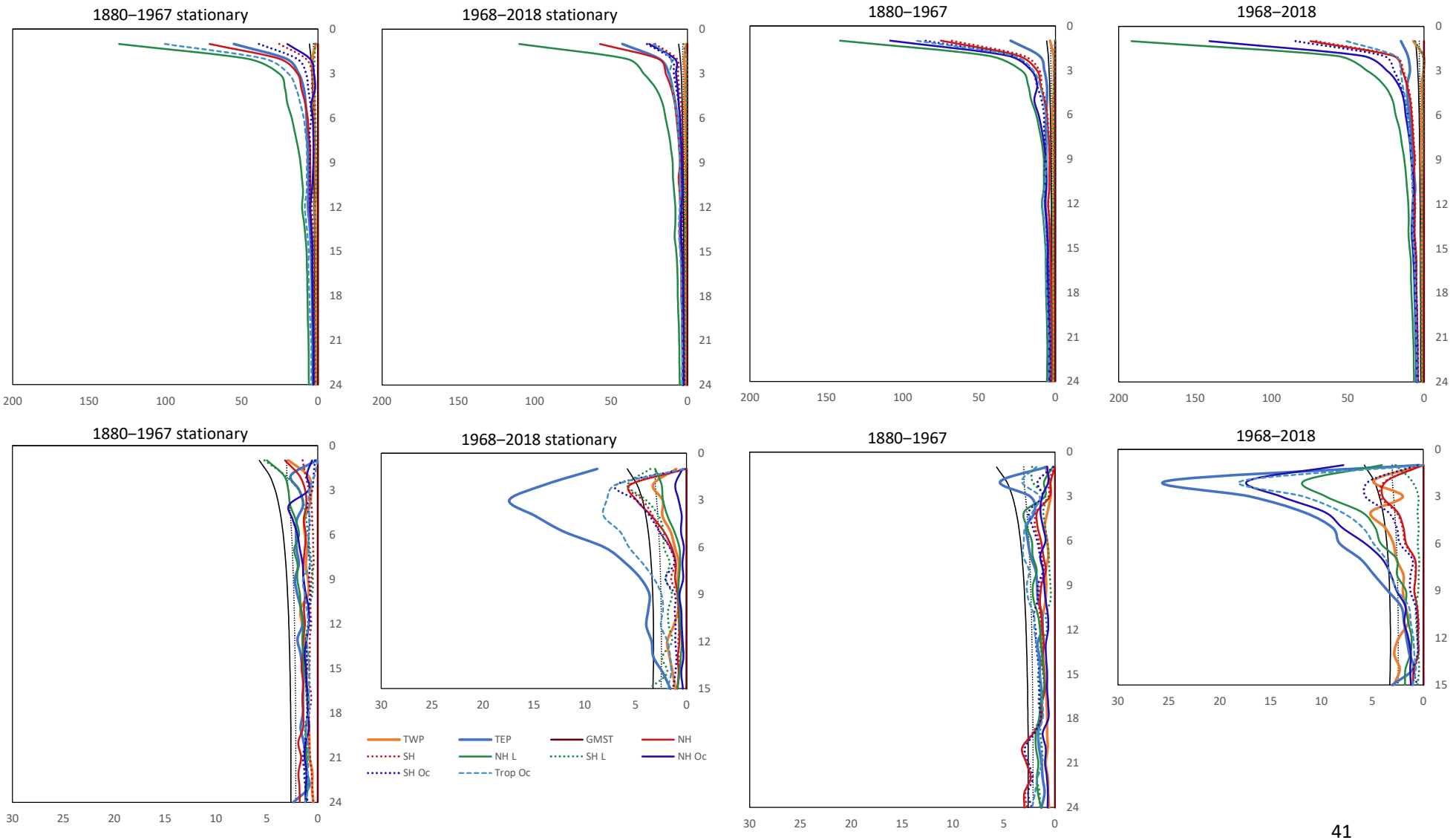

Plate 6: To TWP Monthly (top) and Annual (bottom)

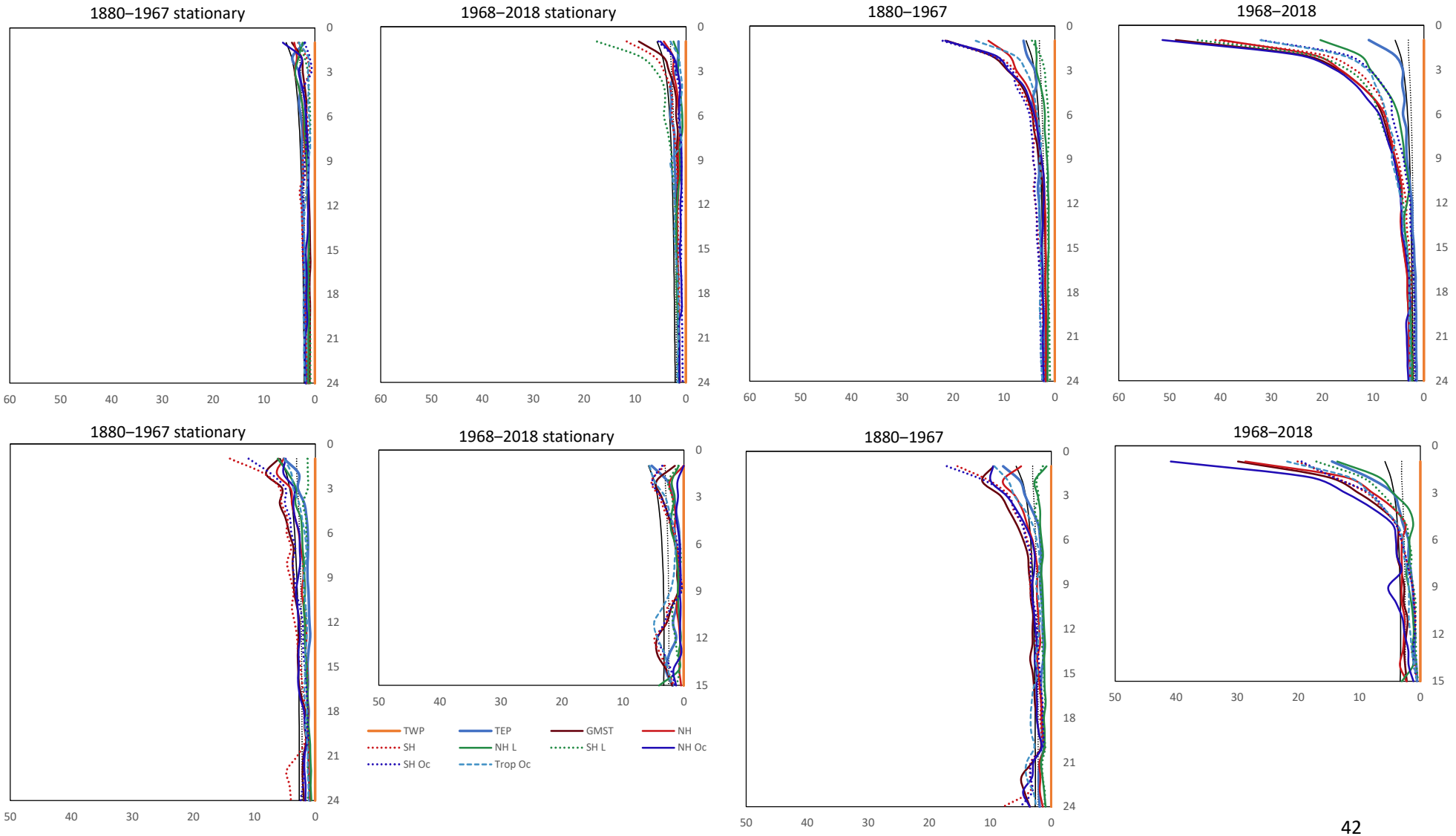

Plate 7: From TWP Monthly (top) and Annual (bottom)

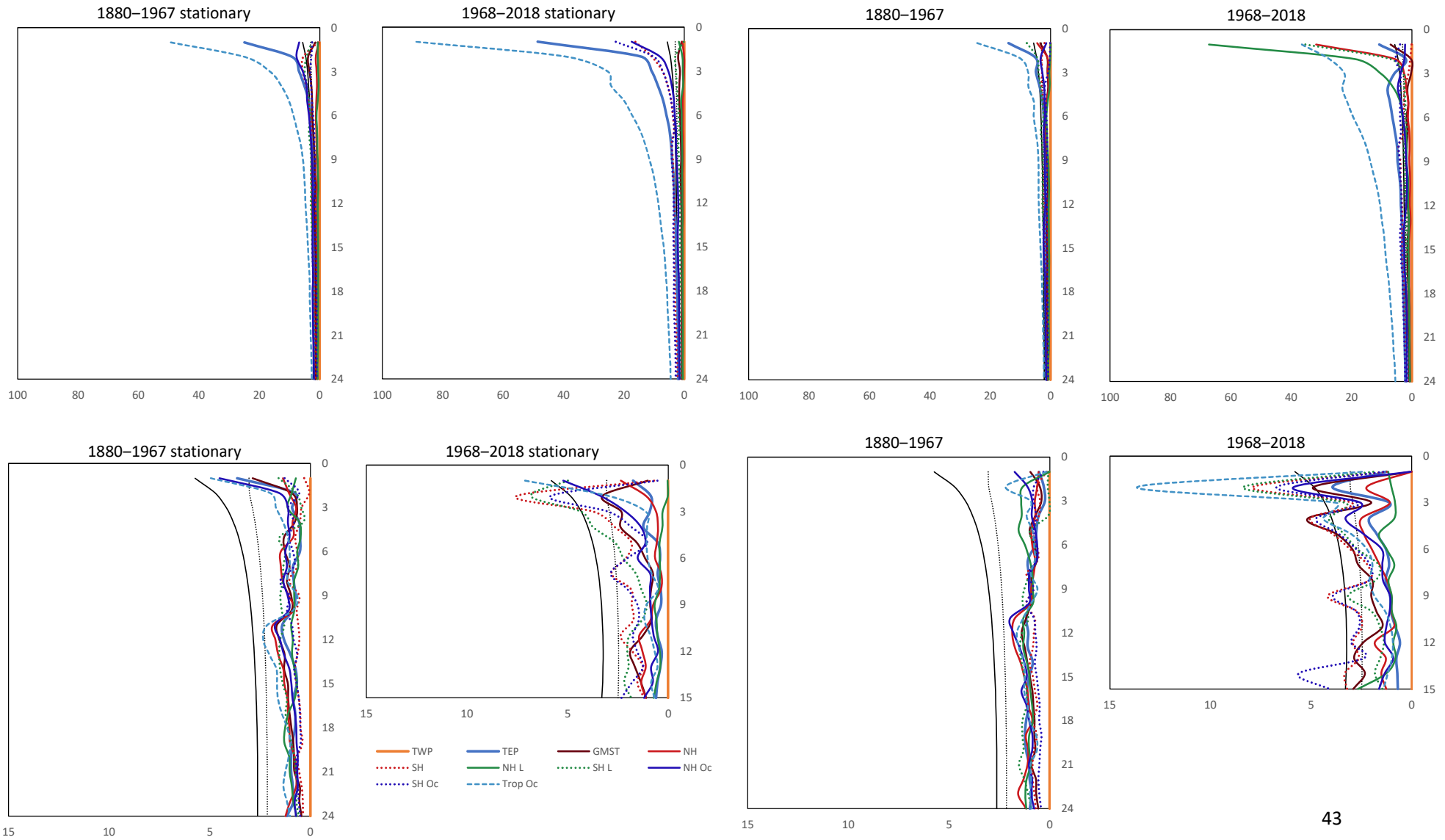

Plate 8: To TEP Monthly (top) and Annual (bottom)

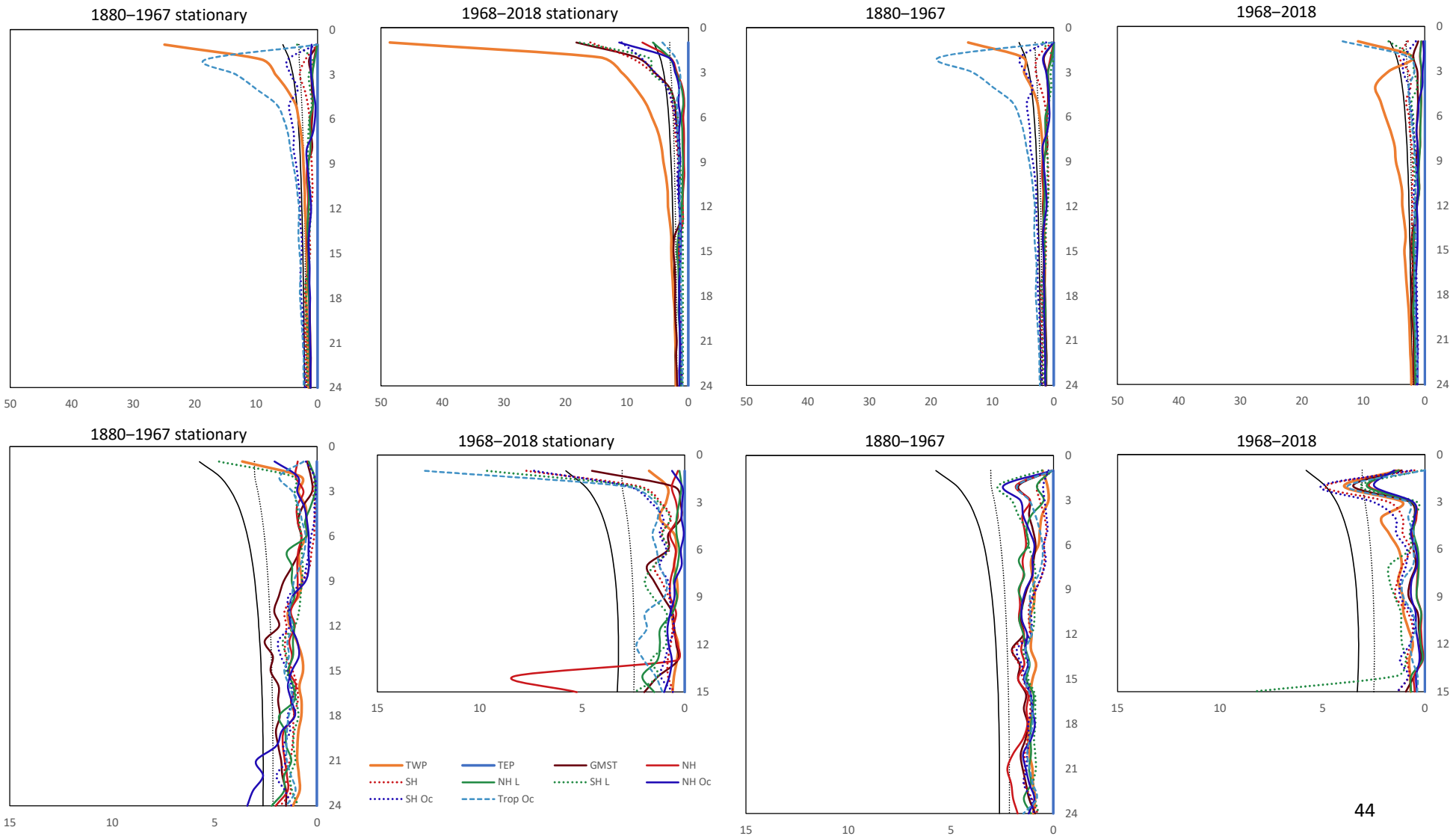

Plate 9: From TEP Monthly (top) and Annual (bottom)

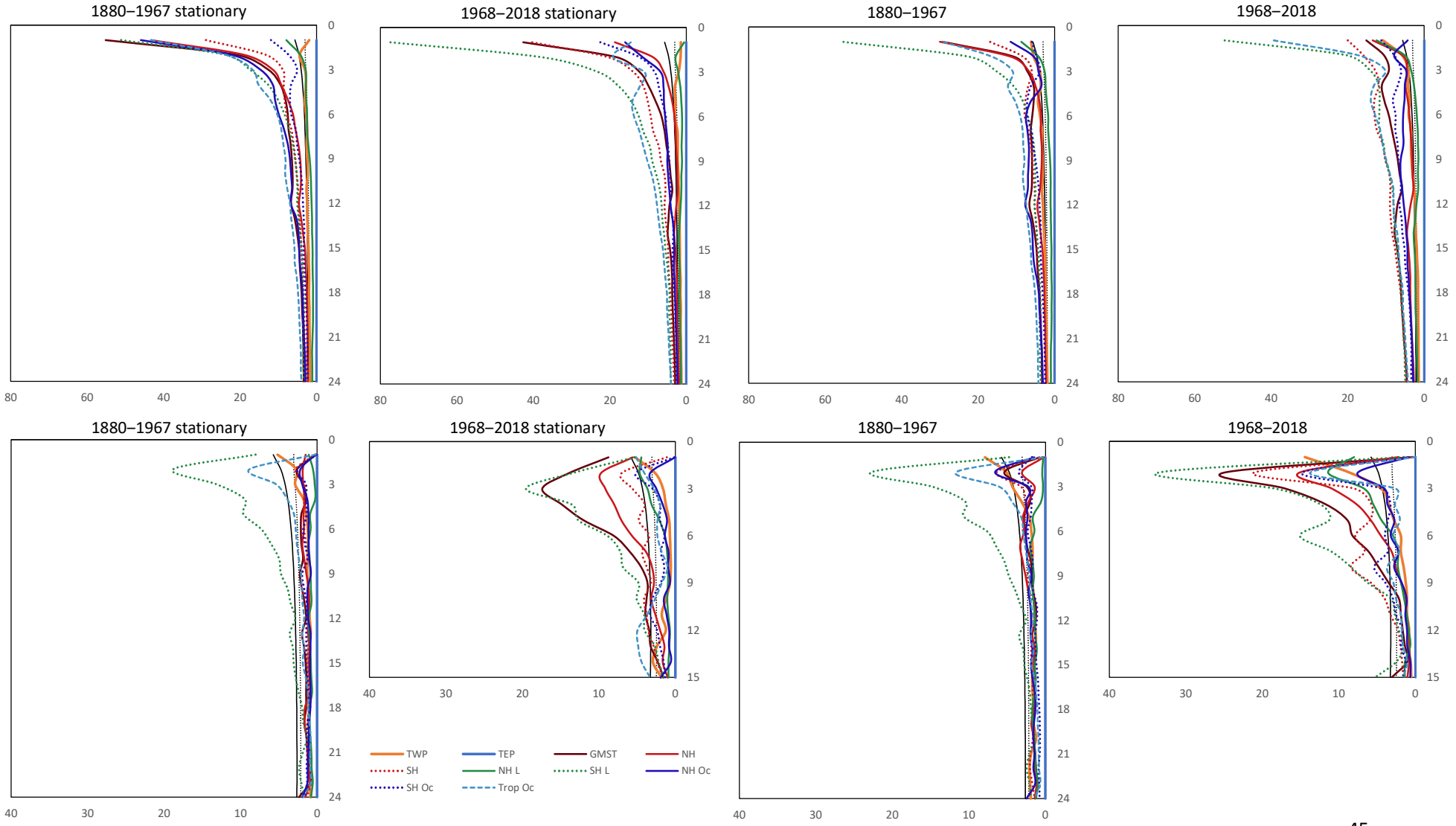

References

Allen, R. J., and Amaya, D. J.: The importance of ENSO/PDO to recent tropical widening, US CLIVAR Variations, 16, 8, 2018.

Beaugrand, G., Conversi, A., Atkinson, A., Cloern, J., Chiba, S., Fonda-Umani, S., Kirby, R. R., Greene, C. H., Goberville, E., Otto, S. A., Reid, P. C., Stemmann, L., and Edwards, M.: Prediction of unprecedented biological shifts in the global ocean, Nat Clim Change, 9, 237-243, http://dx.doi.org/10.1038/s41558-019-0420-1, 2019.

Beaulieu, C., and Killick, R.: Distinguishing trends and shifts from memory in climate data, J Clim, 2018.

Bindoff, N. L., Stott, P. A., AchutaRao, K. M., Allen, M., Gillett, N., Gutzler, D., Hansingo, K., Hegerl, G., Hu, Y., Jain, S., Mokhov, I., Overland, J., Perlwitz, J., Sebbari, R., and Zhang, X.: Detection and Attribution of Climate Change: from Global to Regional, in: Climate Change 2013: The Physical Science Basis. Working Group I contribution to the IPCC 5th Assessment Report, edited by: Stocker, T. F., Qin, D., Plattner, G.-K., Tignor, M., Allen, S. K., Boschung, J., Nauels, A., Xia, Y., Bex, V., and Midgley, P. M., Cambridge University Press, Cambridge and New York, 132, 2013.

Birkel, S. D., Mayewski, P. A., Maasch, K. A., Kurbatov, A. V., and Lyon, B.: Evidence for a volcanic underpinning of the Atlantic multidecadal oscillation, npj Clim Atmos Sci, 1, 24, http://dx.doi.org/10.1038/s41612-018-0036-6, 2018.

Bond, N., Overland, J., Spillane, M., and Stabeno, P.: Recent shifts in the state of the North Pacific, Geophys Res Lett, 30, 2003.

Boucharel, J., Dewitte, B., Garel, B., and Du Penhoat, Y.: ENSO's non-stationary and non-Gaussian character: The role of climate shifts, Nonlinear Processes Geophys, 16, 453-473, 2009.

Boucharel, J., Dewitte, B., Penhoat, Y., Garel, B., Yeh, S.-W., and Kug, J.-S.: ENSO nonlinearity in a warming climate, Clim Dyn, 37, 2045-2065, https://doi.org/10.1007/s00382-011-1119-9, 2011.

Bücher, A., and Dessens, J.: Secular trend of surface temperature at an elevated observatory in the Pyrenees, J Clim, 4, 859-868, 1991.

Buishand, T.: Tests for detecting a shift in the mean of hydrological time series, J Hydrol, 73, 51-69, 1984.

Bureau of Meteorology: An exceptionally dry decade in parts of southern and eastern Australia: October 1996-September 2006, Bureau of Meteorology, Melbourne, 9, 2006.

Caesar, L., Rahmstorf, S., Robinson, A., Feulner, G., and Saba, V.: Observed fingerprint of a weakening Atlantic Ocean overturning circulation, Nature, 556, 191, 2018.

Dickey, D. A., and Fuller, W. A.: Likelihood ratio statistics for autoregressive time series with a unit root, Econometrica, 1057-1072, 1981.

Domonkos, P., Venema, V., Auer, I., Mestre, O., and Brunetti, M.: The historical pathway towards more accurate homogenisation, Adv Sci Res, 8, 45-52, 2012.

Egorova, T., Rozanov, E., Arsenovic, P., Peter, T., and Schmutz, W.: Contributions of natural and anthropogenic forcing agents to the early 20th century warming, Front Earth Sci, 6, 206, 2018.

Enfield, D. B., Mestas-Nuñez, A. M., and Trimble, P. J.: The Atlantic multidecadal oscillation and its relation to rainfall and river flows in the continental US, Geophys Res Lett, 28, 2077-2080, 2001.

Folland, C. K., Boucher, O., Colman, A., and Parker, D. E.: Causes of irregularities in trends of global mean surface temperature since the late 19th century, Sci Adv, 4, eaao5297, https://doi.org/10.1126/sciadv.aao5297, 2018.

Hare, S. R., and Mantua, N. J.: Empirical evidence for North Pacific regime shifts in 1977 and 1989, Prog Oceanogr, 47, 103-145, 2000.

Hawkins, E., and Sutton, R.: Time of emergence of climate signals, Geophys Res Lett, 39, 10.1029/2011gl050087, 2012.

Hegerl, G. C., Brönnimann, S., Schurer, A., and Cowan, T.: The early 20th century warming: Anomalies, causes, and consequences, Wiley Interdiscip Rev Clim Change, 9, e522, 2018.

Hope, P. K., Drosdowsky, W., and Nicholls, N.: Shifts in the synoptic systems influencing southwest Western Australia, Clim Dyn, 26, 751-764, https://doi.org/10.1007/s00382-006-0115-y, 2006.

Huang, B., Banzon, V. F., Freeman, E., Lawrimore, J., Liu, W., Peterson, T. C., Smith, T. M., Thorne, P. W., Woodruff, S. D., and Zhang, H.-M.: Extended Reconstructed Sea Surface Temperature Version 4 (ERSST.v4). Part I: Upgrades and Intercomparisons, J Clim, 28, 911-930, https://doi.org/10.1175/jcli-d-14-00006.1, 2015.
Huang, B., Thorne, P. W., Smith, T. M., Liu, W., Lawrimore, J., Banzon, V. F., Zhang, H.-M., Peterson, T. C., and Menne, M.: Further exploring and quantifying uncertainties for extended reconstructed sea surface temperature (ERSST) version 4 (v4), J Clim, 29, 3119-3142, 2016.
Huang, B., Thorne, P. W., Banzon, V. F., Boyer, T., Chepurin, G., Lawrimore, J. H., Menne, M. J., Smith, T. M., Vose, R. S., and Zhang, H.-M.: Extended reconstructed sea surface temperature, version 5 (ERSSTv5): upgrades, validations, and intercomparisons, J Clim, 30, 8179-8205, 2017.
Jones, R. N.: Detecting and attributing nonlinear anthropogenic regional warming in southeastern Australia, J Geophys Res, 117, D04105, https://doi.org/10.1029/2011jd016328, 2012.
Jones, R. N., and Ricketts, J. H.: Reconciling the signal and noise of atmospheric warming on decadal timescales, Earth Syst Dyn, 8, 177-210, 10.5194/esd-8-177-2017, 2017.
Jones, R. N., and Ricketts, J. H.: Shifts to the new abnormal: riding the waves of climate change AJEM Monograph Series, in review, 2019.
Jones, R. N., and Ricketts, J. H.: The Pacific Ocean heat engine, Earth Syst Dyn, submitted, 2021.
Kirono, D., and Jones, R.: A bivariate test for detecting inhomogeneities in pan evaporation time series, Aust Meteorol Mag, 56, 93-103, 2007.
Lettenmaier, D. P., Wood, E. F., and Wallis, J. R.: Hydro-Climatological Trends in the Continental United States, 1948-88, J Clim, 7, 586-607, https://doi.org/10.1175/1520-0442(1994)007<0586:HCTITC>2.0.CO;2, 1994.
Li, F., Chambers, L., and Nicholls, N.: Relationships between rainfall in the southwest of Western Australia and near global patterns of sea-surface temperature and mean sea-level pressure variability, Aust Meteorol Mag, 54, 23-33, 2005.
Liu, W., Huang, B., Thorne, P. W., Banzon, V. F., Zhang, H.-M., Freeman, E., Lawrimore, J., Peterson, T. C., Smith, T. M., and Woodruff, S. D.: Extended reconstructed sea surface temperature version 4 (ERSST. v4): Part II. Parametric and structural uncertainty estimations, J Clim, 28, 931-951, 2015.
Mahlstein, I., Knutti, R., Solomon, S., and Portmann, R. W.: Early onset of significant local warming in low latitude countries, Environ Res Lett, 6, 034009, 2011.
Mantua, N. J., Hare, S. R., Zhang, Y., Wallace, J. M., and Francis, R. C.: A Pacific interdecadal climate oscillation with impacts on salmon production, Bull Am Meteorol Soc, 78, 1069-1079, 1997.
Maronna, R., and Yohai, V. J.: A bivariate test for the detection of a systematic change in mean, J Am Stat Assoc, 73, 640-645, 1978.
Mayo, D. G.: Error and the Growth of Experimental Knowledge, University of Chicago Press, Chicago, 509 pp., 1996.
Mayo, D. G., and Spanos, A.: Methodology in practice: Statistical misspecification testing, Philosophy of Science, 71, 1007-1025, 2004.
Mayo, D. G.: Evidence as passing severe tests: highly probable versus highly probed hypotheses, in: Scientific Evidence: Philosophical Theories and Applications, edited by: Achinstein, P., John Hopkins University Press, Baltimore and London, 95-127, 2005.
Mayo, D. G., and Spanos, A.: Error and Inference: Recent Exchanges on Experimental Reasoning, Reliability, and the Objectivity and Rationality of science, Cambridge University Press, Cambridge UK, 419 pp., 2010.
Mayo, D. G., and Spanos, A.: Error Statistics, in: Philosophy of Statistics, edited by: Bandyopadhyay, P. S., and Forster, M. R., North-Holland, Amsterdam, 153-198, 2011.
Mayo, D. G.: Statistical Inference as Severe Testing, Cambridge University Press, Cambridge, 486 pp., 2018.
Morice, C. P., Kennedy, J. J., Rayner, N. A., and Jones, P. D.: Quantifying uncertainties in global and regional temperature change using an ensemble of observational estimates: The HadCRUT4 data set, J Geophys Res, 117, D08101, https://doi.org/10.1029/2011JD017187, 2012.

Müller, W. A., Matei, D., Bersch, M., Jungclaus, J. H., Haak, H., Lohmann, K., Compo, G. P., Sardeshmukh, P. D., and Marotzke, J.: A twentieth-century reanalysis forced ocean model to reconstruct the North Atlantic climate variation during the 1920s, Clim Dyn, 44, 1935-1955, 10.1007/s00382-014-2267-5, 2015.
O'Kane, T. J., Matear, R. J., Chamberlain, M. A., and Oke, P. R.: ENSO regimes and the late 1970's climate shift: The role of synoptic weather and South Pacific ocean spiciness, J Comput Phys, 271, 19-38, 2014.
Overland, J., Rodionov, S., Minobe, S., and Bond, N.: North Pacific regime shifts: Definitions, issues and recent transitions, Prog Oceanogr, 77, 92-102, 2008.
Peyser, C. E., Yin, J., Landerer, F. W., and Cole, J. E.: Pacific sea level rise patterns and global surface temperature variability, Geophys Res Lett, 43, 8662–8669, https://doi.org/10.1002/2016GL069401, 2016.
Potter, K.: Illustration of a new test for detecting a shift in mean in precipitation series, Mon Weather Rev, 109, 2040-2045, 1981.
Reid, P. C., and Beaugrand, G.: Global synchrony of an accelerating rise in sea surface temperature, J Mar Biol Assoc UK, 92, 1435-1450, https://doi.org/10.1017/S0025315412000549, 2012.
Reid, P. C., Hari, R. E., Beaugrand, G., Livingstone, D. M., Marty, C., Straile, D., Barichivich, J., Goberville, E., Adrian, R., and Aono, Y.: Global impacts of the 1980s regime shift, Global Change Biol, 22, 682-703, https://doi.org/10.1111/gcb.13106, 2016.
Ribeiro, S., Caineta, J., and Costa, A.: Review and discussion of homogenisation methods for climate data, Phys Chem Earth, 94, 167-179, 2016.
Ricketts, J. H.: A probabilistic approach to climate regime shift detection based on Maronna's bivariate test, The 21st International Congress on Modelling and Simulation (MODSIM2015), Gold Coast, Queensland, Australia, 2015.
Ricketts, J. H., and Jones, R. N.: The multi-step Maronna-Yohai bivariate test for detecting multiple step changes in climate data, Manuscript in preparation, 2016.
Ricketts, J. H.: Understanding the Nature of Abrupt Decadal Shifts in a Changing Climate, Ph D (accepted under revision), Institute of Sustainable Industry and Liveable Cities, Victoria University, Melbourne, 2019.
Rodionov, S.: A sequential method of detecting abrupt changes in the correlation coefficient and its application to Bering Sea climate, Climate, 3, 474-491, 2015.
Santer, B. D., Mears, C., Doutriaux, C., Caldwell, P., Gleckler, P. J., Wigley, T. M. L., Solomon, S., Gillett, N. P., Ivanova, D., Karl, T. R., Lanzante, J. R., Meehl, G. A., Stott, P. A., Taylor, K. E., Thorne, P. W., Wehner, M. F., and Wentz, F. J.: Separating signal and noise in atmospheric temperature changes: The importance of timescale, J Geophys Res, 116, D22105, 10.1029/2011jd016263, 2011.
Sato, M., Hansen, J. E., McCormick, M. P., and Pollack, J. B.: Stratospheric aerosol optical depths, 1850–1990, J Geophys Res, 98, 22987-22994, 1993.
Seidel, D. J., and Lanzante, J. R.: An assessment of three alternatives to linear trends for characterizing global atmospheric temperature changes, J Geophys Res, 109, D14108, https://doi.org/10.1029/2003jd004414, 2004.
Smith, T. M., Reynolds, R. W., Peterson, T. C., and Lawrimore, J.: Improvements to NOAA's historical merged land-ocean surface temperature analysis (1880-2006), J Clim, 21, 2283-2296, 2008.
Štěpánek, P., Zahradníček, P., and Skalák, P.: Data quality control and homogenization of air temperature and precipitation series in the area of the Czech Republic in the period 1961–2007, Adv Sci Res, 3, 23-26, https://doi.org/10.5194/asr-3-23-2009, 2009.
Swingedouw, D., Mignot, J., Ortega, P., Khodri, M., Menegoz, M., Cassou, C., and Hanquiez, V.: Impact of explosive volcanic eruptions on the main climate variability modes, Global Planet Change, 150, 24-45, 2017.
Tian, Y., Ueno, Y., Suda, M., and Akamine, T.: Decadal variability in the abundance of Pacific saury and its response to climatic/oceanic regime shifts in the northwestern subtropical Pacific during the last half century, J Mar Syst, 52, 235-257, 2004.

Vivès, B., and Jones, R. N.: Detection of Abrupt Changes in Australian Decadal Rainfall (1890-1989), CSIRO Atmospheric Research, Melbourne, 54, 2005.
Vose, R. S., Arndt, D., Banzon, V. F., Easterling, D. R., Gleason, B., Huang, B., Kearns, E., Lawrimore, J. H., Menne, M. J., Peterson, T. C., Reynolds, R. W., Smith, T. M., Williams, C. N., and Wuertz, D. B.: NOAA's Merged Land–Ocean Surface Temperature Analysis, Bull Am Meteorol Soc, 93, 1677-1685, https://doi.org/10.1175/BAMS-D-11-00241.1, 2012.
Wang, J., Xu, C., Hu, M., Li, Q., Yan, Z., and Jones, P.: Global land surface air temperature dynamics since 1880, Int J Climatol, 38, e466-e474, 2018.
Xue, Y., Smith, T. M., and Reynolds, R. W.: Interdecadal changes of 30-yr SST normals during 1871–2000, J Clim, 16, 1601-1612, 2003.
Zhang, W., Li, J., and Jin, F. F.: Spatial and temporal features of ENSO meridional scales, Geophys Res Lett, 36, L15605, https://doi.org/10.1029/2009GL038672, 2009.
Zhang, Y., Wallace, J. M., and Battisti, D. S.: ENSO-like interdecadal variability: 1900–93, J Clim, 10, 1004-1020, 1997.
Zivot, E., and Andrews, D. W.: Further Evidence on the Great Crash, the Oil-Price Shock, and the Unit-Root Hypothesis, Journal of Business & Economic Statistics, 1992.